Seismic Structure, Crustal Architecture and Tectonic Evolution of the Anatolian–African Plate Boundary and the Cenozoic Orogenic...

Chapter *in* Geological Society London Special Publications · December 2009

DOI: 10.1144/SP327.8

2 authors:

Yildirim Dilek
Miami University

Eric Sandvol
University of Missouri

Seismic structure, crustal architecture and tectonic evolution of the Anatolian–African Plate Boundary and the Cenozoic Orogenic Belts in the Eastern Mediterranean Region

YILDIRIM DILEK[1*] & ERIC SANDVOL[2]

[1]*Department of Geology, Miami University, Oxford, OH 45056, USA*

[2]*Department of Geology Sciences, University of Missouri-Columbia, Columbia, MO 65211, USA*

**Corresponding author (e-mail: dileky@muohio.edu)*

Abstract: The modern Anatolian–African plate boundary is represented by a north-dipping subduction zone that has been part of a broad domain of regional convergence between Eurasia and Afro–Arabia since the latest Mesozoic. A series of collisions between Gondwana-derived ribbon continents and trench-roll-back systems in the Tethyan realm produced nearly East–West-trending, subparallel mountain belts with high elevation and thick orogenic crust in this region. Ophiolite emplacement, terrane stacking, high-P and Barrovian metamorphism, and crustal thickening occurred during the accretion of these microcontinents into the upper plates of Tethyan subduction roll-back systems during the Late Cretaceous–Early Eocene. Continued convergence and oceanic lithospheric subduction within the Tethyan realm were punctuated by slab breakoff events following the microcontinental accretion episodes. Slab breakoff resulted in asthenospheric upwelling and partial melting, which facilitated post-collisional magmatism along and across the suture zones. Resumed subduction and slab roll-back-induced upper plate extension triggered a tectonic collapse of the thermally weakened orogenic crust in Anatolia in the late Oligocene–Miocene. This extensional phase resulted in exhumation of high-P rocks and medium- to lower-crustal material leading to the formation of metamorphic core complexes in the hinterland of the young collision zones. The geochemical character of the attendant magmatism has progressed from initial shoshonitic and high-K calc-alkaline to calc-alkaline and alkaline affinities through time, as more asthenosphere-derived melts found their way to the surface with insignificant degrees of crustal contamination. The occurrence of discrete high-velocity bodies in the mantle beneath Anatolia, as deduced from lithospheric seismic velocity data, supports our Tethyan slab breakoff interpretations. Pn velocity and Sn attenuation tomography models indicate that the uppermost mantle is anomalously hot and thin, consistent with the existence of a shallow asthenosphere beneath the collapsing Anatolian orogenic belts and widespread volcanism in this region. The sharp, north-pointing cusp (Isparta Angle) between the Hellenic and Cyprus trenches along the modern Anatolian–African plate boundary corresponds to a subduction-transform edge propagator (STEP) fault, which is an artifact of a slab tear within the downgoing African lithosphere.

Introduction

The present-day geodynamics of the eastern Mediterranean region is controlled by the relative motions of three major plates, Eurasia, Africa and Arabia, and much of the resulting deformation occurs at their boundaries (Fig. 1; Westaway 1994; Jolivet & Faccenna 2000; McClusky *et al.* 2000; Doglioni *et al.* 2002; Dilek 2006; Reilinger *et al.* 2006). The convergence rate between Africa and Eurasia is >40 mm a^{-1} across the Hellenic Trench but decreases to <10 mm a^{-1} across the Cyprus trench to the east (McClusky *et al.* 2000; Doglioni *et al.* 2002; Wdowinski *et al.* 2006) as a result of the subduction of the Eratosthenes seamount beneath Cyprus (Robertson 1998). The Arabia–Eurasia convergence across the Bitlis–Zagros suture zone has been estimated to be *c.* 16 mm a^{-1} based on global positioning system measurements of present-day central movements in this collision zone (Reilinger *et al.* 1997, 2006). These differential northward motions of Africa (<10 mm a^{-1}) and Arabia (16 mm a^{-1}) with respect to Eurasia are accommodated along the sinistral Dead Sea fault zone (Fig. 1b). The Anatolian microplate north of these convergent plate boundaries is moving SW with respect to Eurasia (Fig. 1a) at *c.* 30 mm a^{-1} along the North and East Anatolian fault zones (Reilinger *et al.* 1997) and is undergoing complex internal deformation via mainly strike-slip and normal faulting. This deformation has resulted in the extensional collapse of the young orogenic crust, which developed during a series of collisional events in the region (Dewey *et al.* 1986; Dilek &

From: MURPHY, J. B., KEPPIE, J. D. & HYNES, A. J. (eds) *Ancient Orogens and Modern Analogues.* Geological Society, London, Special Publications, **327**, 127–160.
DOI: 10.1144/SP327.8 0305-8719/09/$15.00

(a)

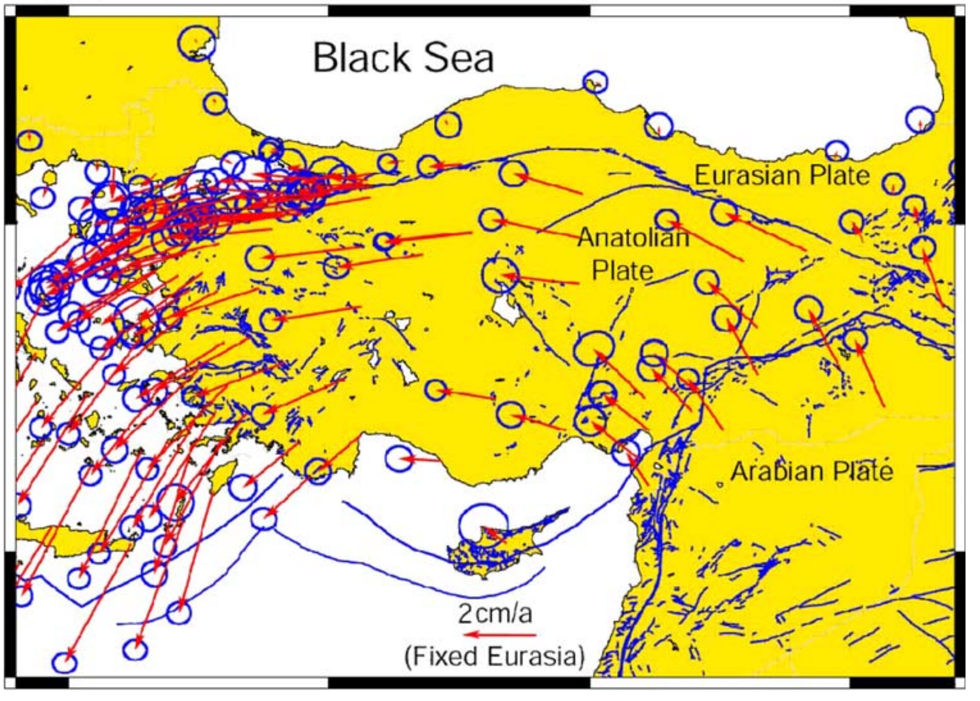

Fig. 1. (**a**) GPS velocity vectors for Anatolia and the Aegean Sea plotted in a Eurasia fixed reference frame (modified from Reilinger *et al.* 1997). The major mapped faults for western Anatolia are shown as lines and circles. **(b)** Tectonic map of the Aegean and eastern Mediterranean region showing the main plate boundaries, major suture zones, fault systems and tectonic units. Thick, white arrows depict the direction and magnitude (mm a^{-1}) of plate convergence; grey arrows mark the direction of extension (Miocene–Recent). Orange and purple delineate Eurasian and African plate affinities, respectively. Key to lettering: BF, Burdur fault; CACC, Central Anatolian Crystalline Complex; DKF, Datça–Kale fault (part of the SW Anatolian Shear Zone); EAFZ, East Anatolian fault zone; EF, Ecemis fault; EKP, Erzurum–Kars Plateau; IASZ, Izmir–Ankara suture zone; IPS, Intra–Pontide suture zone; ITS, Inner–Tauride suture; KF, Kefalonia fault; KOTJ, Karliova triple junction; MM, Menderes massif; MS, Marmara Sea; MTR, Maras triple junction; NAFZ, North Anatolian fault zone; OF, Ovacik fault; PSF, Pampak–Sevan fault; TF, Tutak fault; TGF, Tuzgölü fault; TIP, Turkish–Iranian plateau (modified from Dilek 2006).

Moores 1990; Yilmaz 1990), giving way to the formation of metamorphic core complexes and intracontinental basins (Bozkurt & Park 1994; Dilek & Whitney 2000; Jolivet & Faccenna 2000; Okay & Satir 2000; Doglioni *et al.* 2002; Ring & Layer 2003). Extensional deformation of the young orogenic belts has been accompanied by magmatism with varying geochemical fingerprints. The cause-effect relations of the spatial and temporal interplay between post-collisional extension and magmatism in the eastern Mediterranean region have been a subject of intense scrutiny and interdisciplinary research over the last twenty years.

The modern collision zone between the Anatolian and African plates is an excellent natural laboratory to study the last stages of subduction, subduction roll-back processes, and accretionary events prior to the onset of continental collision. The 1000 km-long convergent plate boundary between these two plates comprises two separate arcs: the Hellenic and the Cyprean (Fig. 1). The intersection of these two subduction zones occurs in a sharp bend, the Isparta Angle (IA), in the Tauride block. The Hellenic arc is characterized by a relatively steep, retreating subduction, whereas the Cyprean arc appears to involve a shallow subduction with two major seamounts (the Eratosthenes and Anixamander) impinging on the trench (Kempler & Ben-Avraham 1987; Zitter *et al.* 2003).

In this paper we examine the Cenozoic evolution of the African–Anatolian plate boundary utilizing seismic tomography, and use our observations and interpretations from this modern subduction-collision driven plate boundary to derive

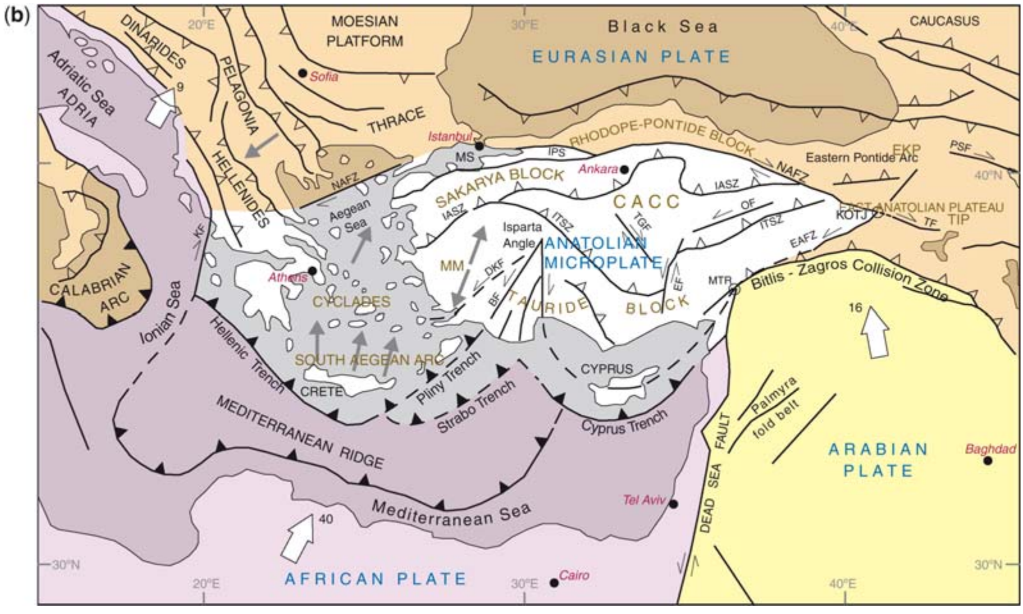

Fig. 1. (*Continued*)

conclusions for the geodynamic evolution and mantle dynamics of the young (Cenozoic) orogenic belts in Anatolia. Our tomographic models of the upper mantle beneath Anatolia and the Aegean Sea support the existence of two discrete high-velocity regions. These may be indicative of two separate slab breakoff events that have occurred during the subduction of the Tethyan oceanic lithosphere. We use our own geological observations and data, and the extant literature to re-interpret the collision-driven tectonic evolution of the western, central and eastern Anatolian orogenic belts and to provide an overview of their crustal architecture.

Seismic structure of the collision zones in Anatolia and its environs

Lithospheric seismic velocity structure

Seismic images of the mantle provide important information on the current state of the lithosphere and asthenosphere in the eastern Mediterranean region. In particular, the location of possible preserved slabs beneath the Anatolian plate could prove useful in understanding the evolution of the African–Anatolian plate boundary and the geodynamics of the Cenozoic orogenic belts in the region. In many models, however, the uppermost mantle picture is not well resolved in regions lacking fairly dense station coverage. This is certainly true for much of western and central Anatolia. Pn tomography, however, offers an important snapshot of the lithospheric mantle seismic velocity structure, even in regions with sparse station coverage. Similarly, seismic phase attenuation can also indicate the state of the lithospheric mantle. Specifically, the regional seismic phase Sn is very sensitive to lithospheric mantle temperature anomalies (e.g. Molnar & Oliver 1969; Rodgers *et al.* 1995; Sandvol *et al.* 2001). Sn attenuation and Pn velocity are, therefore, two complementary and independent measures of the state of the uppermost mantle. Using these two models we find that the majority of the Anatolian plate is underlain by highly attenuating and seismically slow material (Figs 2 & 3). The two images from these independent datasets confirm that the Anatolian lithosphere is hot and most probably relatively thin.

Pn velocity tomography with an anisotropy component shows two scales of low Pn velocity anomalies (Fig. 2). First, a broader scale (*c.* 500 km) low (<7.8 km/s) Pn velocity anomaly underlies northwestern Iran, eastern Anatolia, the Caucasus, most of the Anatolian plate, and the northern Aegean Sea. These broad-scale low Pn velocity anomalies occupy regions within the Eurasian side of the Eurasia–Arabia collision zone. In central Iran, fast Pn velocities appear to extend beyond the Zagros suture line, while in northwestern Iran and eastern Turkey the high Pn velocities are limited to the region immediately south of the Bitlis–Zagros suture zone and the Tauride block.

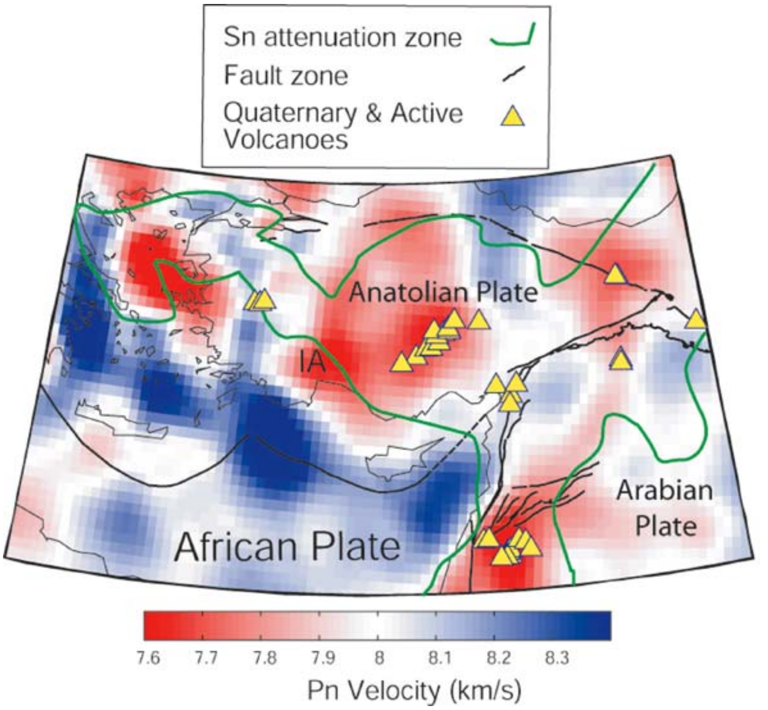

Fig. 2. Pn travel time tomography using all available phase data in the Middle East (Al-Lazki *et al.* 2004). The green line is the approximate boundary of a zone of Sn blockage (Fig. 3). Note the anomalously low Pn velocities along southern Turkey especially in the vicinity of the Isparta Angle (IA).

The Sn attenuation tomography model reveals regions of blocked and attenuated Sn (Fig. 3; Gök *et al.* 2000, 2003). In the southern Aegean Sea, a volcanic arc is present north of Crete and parallel to the Hellenic arc and Sn is attenuated. In the northern Aegean Sea, there is a high attenuating Sn zone with low upper mantle velocities (Al-Lazki *et al.* 2003) and Sn is partially attenuated or inefficient in northern Greece. Conversely, there is efficient Sn throughout most of Greece. In the Black Sea there is a very abrupt transition from efficient to blocked Sn regions. Efficient Sn is observed for paths within the eastern Arabian plate and the Zagros fold-and-thrust belt. An efficient zone is also seen at the northern part of the fold-and-thrust belt in the northwestern corner of the Iranian plateau. However, this region might be distorted because of smearing (Fig. 2). The Pn velocity tomography of Al-Lazki *et al.* (2003) shows higher Pn velocities for a smaller portion of the same region. Clearly, Sn is blocked throughout the Anatolian plateau, whereas it propagates efficiently within the eastern part of the Bitlis–Zagros suture zone. Sn also propagates efficiently through the Black Sea and the Mediterranean Sea. In general there is a strong correlation between Quaternary volcanism and Sn blockage. Throughout the entire Anatolian plateau and northern Arabia, young basaltic volcanism correlates well with regions of high Sn attenuation (Fig. 3).

In the easternmost portion of the model, inefficient Sn is observed in the Greater Caucasus. Throughout most of the Lesser Caucasus, Sn is highly attenuated. Sn is observed as efficient in the western section of the Pontides and inefficient in the eastern Pontides. In western Anatolia, there are some inefficient Sn regions, unlike the regions of Sn blockage observed in eastern Anatolia.

The results of Sn attenuation tomography are consistent with those of Pn tomography, both indicating that the uppermost mantle beneath much of Anatolia is anomalously hot and thin. In western Anatolia, we observe complicated patterns of Sn attenuation, except for the Aegean Sea volcanic arc. A region of clear and distinctly higher Sn attenuation is observed north of the Hellenic trench that is an area of active arc-backarc extension above the northward subducting African plate. Numerous studies have found low velocities in the upper mantle that are consistent with the Sn efficiency results (e.g. Spakman *et al.* 1993; Alessandrini *et al.* 1997; Piromallo & Morelli 2003). The

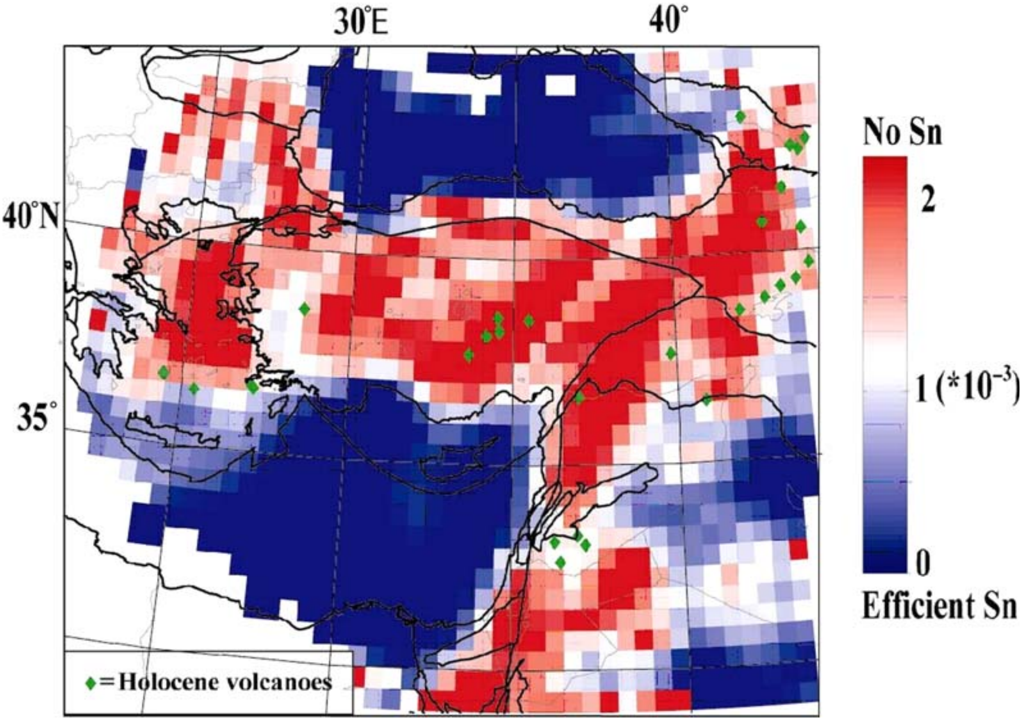

Fig. 3. Tomographic map of Sn attenuation within the Anatolian plate and surrounding regions. Green diamonds indicate Holocene volcanoes. Note good correlation between the Pn tomographic image (Fig. 2) and Sn attenuation, both indicating that the lithosphere is thin and hot throughout most of the Anatolian plate (Gök *et al.* 2003).

partial attenuation of Sn in the northern part of the Aegean Sea is related to active extensional deformation in the backarc setting. The continental shortening in NW Greece and Albania does not allow the rotation of the western margin of the region and leads to east–west shortening and north–south extension as the southern Aegean margin moves towards the Hellenic trench. The efficient Sn zone in part of Greece might be related to the subducting slab.

Upper mantle and transition zone

There have been many tomographic P-wave, S-wave and bulk sound velocity models constructed for the upper mantle of the eastern Mediterranean region (Spakman *et al.* 1993; Bijwaard & Spakman 2000; Kárason & Van Der Hilst *et al.* 2001; Wortel & Spakman 1992, 2000; Widiyantoro *et al.* 2004). Features common to many of these models support their reliability. For example, along the Hellenic trench, the subducted slab of largely oceanic lithosphere of the African plate stands out as a relatively steeply dipping structure with a strong high-velocity P-wave (Fig. 4). This anomaly extends to depths that exceed the intermediate depth seismicity in the region, a result that concurs with the previous images of deep subduction in this region (e.g. Spakman *et al.* 1988, 1993; Wortel & Spakman 1992). In contrast, the image of the Cyprean slab velocity anomaly is much weaker in most tomographic models (e.g. Widiyantoro *et al.* 2004; Fig. 5). This largely aseismic structure is located near the Vrancea seismic zone and may be related to an earlier episode in the multi-stage closing history of the Tethyan seaways (Dilek *et al.* 1999*a*, 2008). This structure is, however, less obvious in the Kárason & Van der Hilst (2001) model, and further investigation is necessary.

We can use the upper mantle velocity structure to infer the number of slab breakoff events that have occurred in the Neogene. Beneath the Eastern Mediterranean, Aegean Sea and Anatolian plate, the seismic velocity structure of the mantle transition zone is characterized by a number of discrete high-velocity bodies. Current global and regional models for the Eastern Mediterranean clearly show the continuation of subducting ocean lithosphere into the lower mantle along the Hellenic trench and its flattening out at the 660 km discontinuity. Many

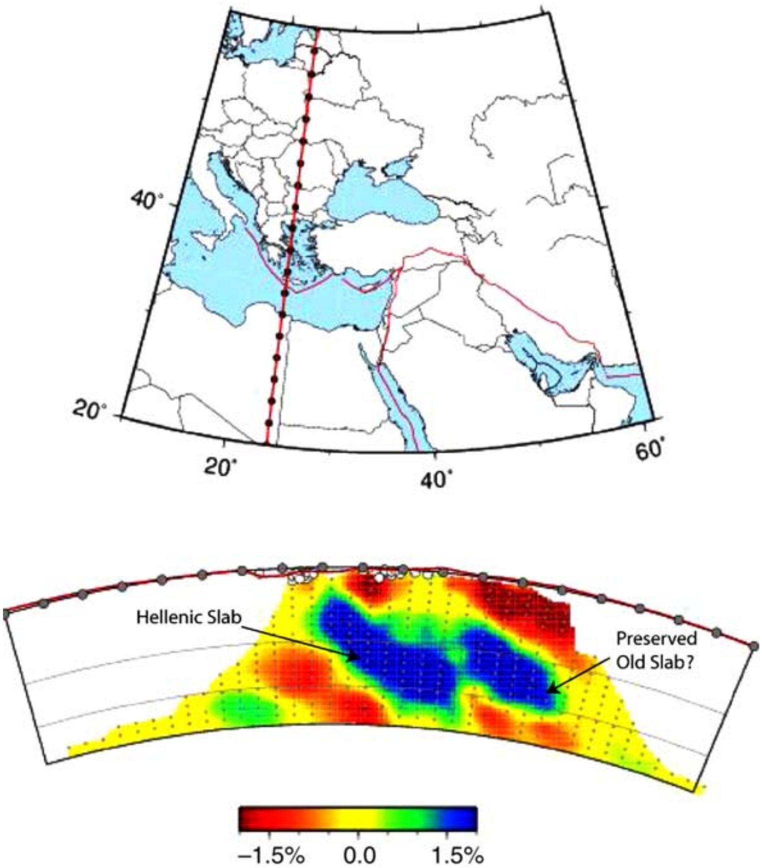

Fig. 4. Seismic tomography cross-section of the mantle to a depth of 800 km in the Aegean region mantle taken perpendicular to the Hellenic trench. Colours display the percentage deviation of seismic wave speed. Negative (positive) anomalies likely represent predominantly higher (lower) temperatures than average. Dashed lateral lines in the section depict the mantle discontinuities at 410 km and 660 km depths. See text for discussion.

(not all) of the newer tomographic models, however, show that there are two high-velocity bodies in the mantle transition zone beneath the Aegean Sea (e.g. Kárason 2002; Widiyantoro *et al.* 2004; Fig. 4).

Pn and Sn tomographic models provide no evidence for an attached slab along any of the suture zones within the Anatolian plate. Nor do they provide evidence of a very shallow/flat slab underlying southern Anatolia, as suggested by some researchers (i.e. Doglioni *et al.* 2002; Agostini *et al.* 2007). Many teleseismic velocity models show a relatively shallow high-velocity anomaly underlying much of central and, in some cases, northern Anatolia. This is in contrast to the uppermost mantle images that suggest that the Anatolian lithosphere is hot and possibly thin. This might suggest that the flat or shallow slab of the Cyprean subduction zone may not be in direct contact with the Anatolian lithosphere, and may extend almost to the North Anatolian Fault Zone (Fig. 5). It still remains unclear as to what role the subducting Cyprean lithosphere had in the very recent uplift of the high topography in the Cyprean back arc (i.e. the Tauride block).

The Isparta Angle

The Isparta Angle (IA) occurs at the intersection between the Cyprean (east) and Hellenic (west) arcs in the western end of the Tauride block (Fig. 1b). Palaeomagnetic investigations suggest that there has been very little rotation of the IA in the last 10 my (Tatar *et al.* 2002). Seismogenic deformation along the Hellenic arc indicates a transition from compressional to normal faulting near the Isparta Angle. On the other hand, the few available focal mechanisms along the westernmost Cyprean arc are more consistent with thrust

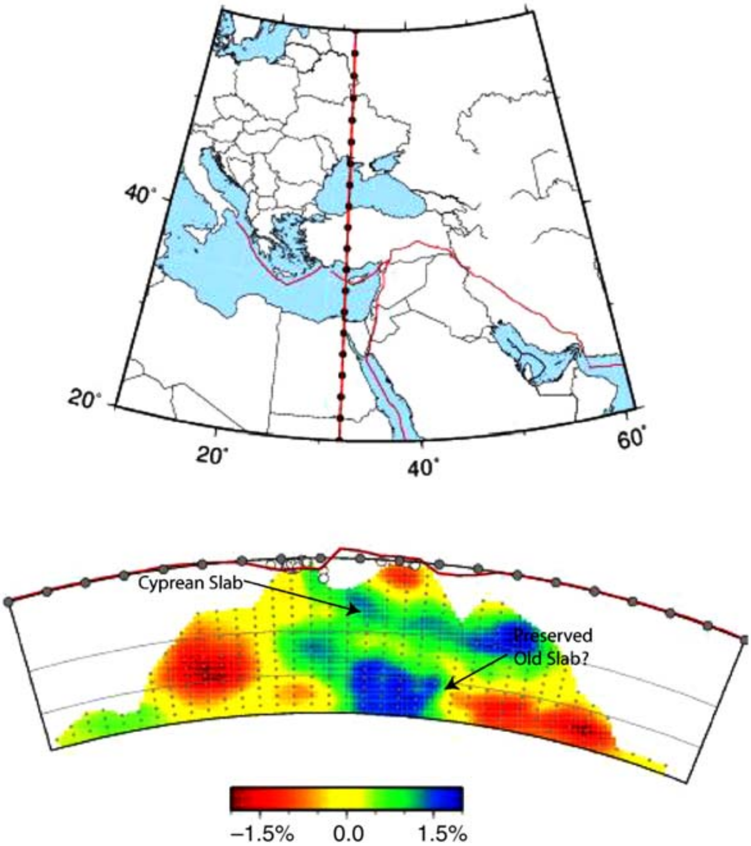

Fig. 5. Seismic tomography cross-section of the mantle to a depth of 800 km in the Central Anatolian region mantle taken perpendicular to the Cyprus trench. Colours display the percentage deviation of seismic wave speed. Negative (positive) anomalies likely represent predominantly higher (lower) temperatures than average. Dashed lateral lines in the section depict the mantle discontinuities at 410 km and 660 km depths. See text for discussion.

faulting. The GPS velocity vectors of McClusky *et al.* (2000) suggest that the lithosphere within the IA is moving independently of the rest of the Anatolian plate and that it may be attached to the African plate or to a piece of it (Barka & Reilinger 1997; McClusky *et al.* 2000).

The sharp cusp between the Hellenic and Cyprus trenches (Fig. 1b) and the significant differences in the convergence velocities of the African lithosphere at these trenches (*c*. 40 vs <10 mm a^{-1} at the Hellenic and Cyprus trenches, respectively) are likely to have resulted in a lithospheric tear in the downgoing African plate that allowed the asthenospheric mantle to rise beneath SW Anatolia (Fig. 6; Doglioni *et al.* 2002; Agostini *et al.* 2007; Dilek & Altunkaynak 2008). This scenario is analogous to lithospheric tearing at subduction-transform edge propagator (STEP) faults described by Govers & Wortel (2005) from the Ionian and Calabrian arcs, the New Hebrides trench, the southern edge of the Lesser Antilles trench, and the northern end of the South Sandwich trench. In all these cases, STEP faults propagate in a direction opposite to the subduction direction, and asthenospheric upwelling occurs behind and beneath their propagating tips. This upwelling induces decompressional melting of shallow asthenosphere, leading to linearly distributed alkaline magmatism younging in the direction of tear propagation.

The North–South-trending potassic and ultrapotassic volcanic fields stretching from the Kirka and Afyon-Suhut region in the north to the Isparta–Gölcük area in the south (Fig. 7) shows an age progression from 21–17 to 4.6–4.0 Ma (Yagmurlu *et al.* 1997; Alici *et al.* 1998; Savaşçin & Oyman 1998; Francalanci *et al.* 2000; Kumral *et al.* 2006; Çoban & Flower 2006; Dilek & Altunkaynak 2007). This distribution of the potassic and ultrapotassic volcanic rocks in SW Anatolia is consistent with a progressive migration of their melt source

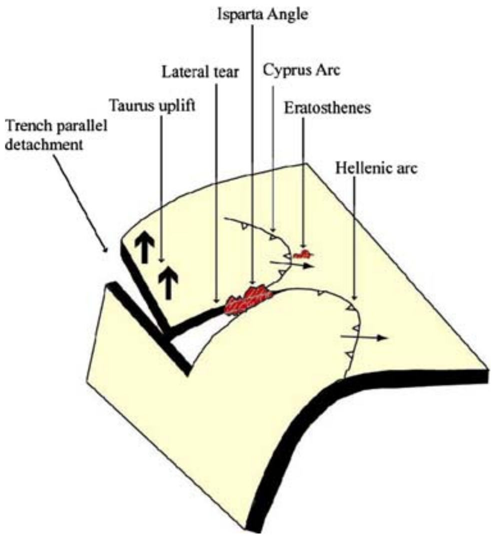

Fig. 6. A cartoon illustrating the development of a slab tear or subduction transform edge propagator (STEP) fault beneath the Tauride block and the positions of subducting African lithosphere beneath the Cyprean and Hellenic arcs (after Barka & Reilinger 1997). Evidence for a southward increase in the age of volcanism is consistent with model (Yagmurlu *et al.* 1997; Savasçin & Oyman 1998; Dilek & Altunkaynak 2008). Also, the presence of ignimbrites is consistent with asthenospheric upwelling leading to widespread crustal melting.

towards the south and supports a STEP model for their origin (Fig. 6; Dilek & Altunkaynak 2008). Asthenospheric low velocities detected through Pn tomographic imaging in this region (Al-Lazki *et al.* 2004) also support the existence of shallow asthenosphere beneath the IA at present.

Regional geology of western Anatolia

The Aegean province is situated in the upper plate of a north-dipping subduction zone at the Hellenic trench (Fig. 1b) and is considered to have evolved as a backarc environment above this subduction zone (Le Pichon & Angelier 1979; Jolivet 2001; Faccenna *et al.* 2003; van Hinsbergen *et al.* 2005). The slab retreat rate of the subducting African lithosphere has been larger than the absolute velocity of the Eurasian upper plate, causing net *c*. North–South extension in the Aegean region since the early Miocene (Jolivet *et al.* 1994; Jolivet & Faccenna 2000; Faccenna *et al.* 2003; Ring & Layer 2003; Dilek & Altunkaynak 2008). Since then, the thrust front associated with this subduction zone and its slab retreat has migrated from the Hellenic trench (south of Crete) to the south of the Mediterranean Ridge (Jolivet & Faccenna 2000; Le Pichon *et al.* 2003). Backarc extension in the Aegean region appears to have started at *c*. 25 Ma, long before the onset of the Arabian collision-driven southwestward displacement of the Anatolian microplate in the late Miocene (Barka & Reilinger 1997; Jolivet & Faccenna 2000).

The continental crust making up the upper plate of the Hellenic subduction zone south of the North Anatolian fault is composed of the Sakarya and the Anatolide–Tauride continental blocks (Fig. 7). These two microcontinents are separated by the Izmir–Ankara suture zone, which is marked by Tethyan ophiolites and associated tectonic units. The basement of the Anatolide block is composed mainly of the Menderes massif, which is intruded and overlain by Cenozoic granitoid plutons and extrusive rocks; Lower Miocene and younger sedimentary rocks of a series of extensional basins overlie the high-grade metamorphic rocks of the Menderes massif (Bozkurt 2003; Purvis & Robertson 2004; Oner & Dilek 2007).

Sakarya continent

The Sakarya continent consists of a Palaeozoic crystalline basement with its Permo–Carboniferous sedimentary cover and Permo–Triassic ophiolitic and rift or accretionary-type mélange units (Karakaya complex) that collectively form a composite continental block (Tekeli 1981; Okay *et al.* 1996). The Sakarya continental rocks and the ophiolitic units of the Izmir–Ankara suture zone (IASZ) are

Fig. 7. Geological map of western Anatolia and the eastern Aegean region, showing the distribution of suture zones, ophiolite complexes, major Cenozoic igneous provinces discussed in this paper, and the salient fault systems. Menderes and Kazdag (KDM) massifs represent metamorphic core complexes with exhumed lower continental crust. Izmir–Ankara suture zone (IASZ) marks the collision front between the Sakarya continental block to the north and the Anatolide–Tauride block to the south. The Intra–Pontide suture zone (IPSZ) marks the collision front between the Sakarya continent to the south and the Rhodope–Pontide block to the north. The Eocene and Oligo–Miocene granitoids (shown in red) represent the post-collisional (post-Eocene) and/or extensional magmatism in the region. Key to lettering of these granitoids: AG, Alasehir; BG, Baklan; CGD, Çataldag; EP, Egrigöz; GBG, Göynükbelen; GYG, Gürgenyayla; IGD, Ilica; KG, Kozak; KOP, Koyunoba; OGD, Orhaneli; TG, Turgutlu; TGD, Topuk; SG, Salihli. Much of western Anatolia is covered by Cenozoic volcanic rocks intercalated with terrestrial deposits. Key to lettering of major fault systems: AF, Acigöl fault; BFZ, Burdur fault zone; DF, Datça fault; IASZ, Izmir–Ankara suture zone; IPSZ, Intra–Pontide suture zone; KF, Kale fault; NAFZ, North Anatolian fault zone; SWASZ, SW Anatolian shear zone.

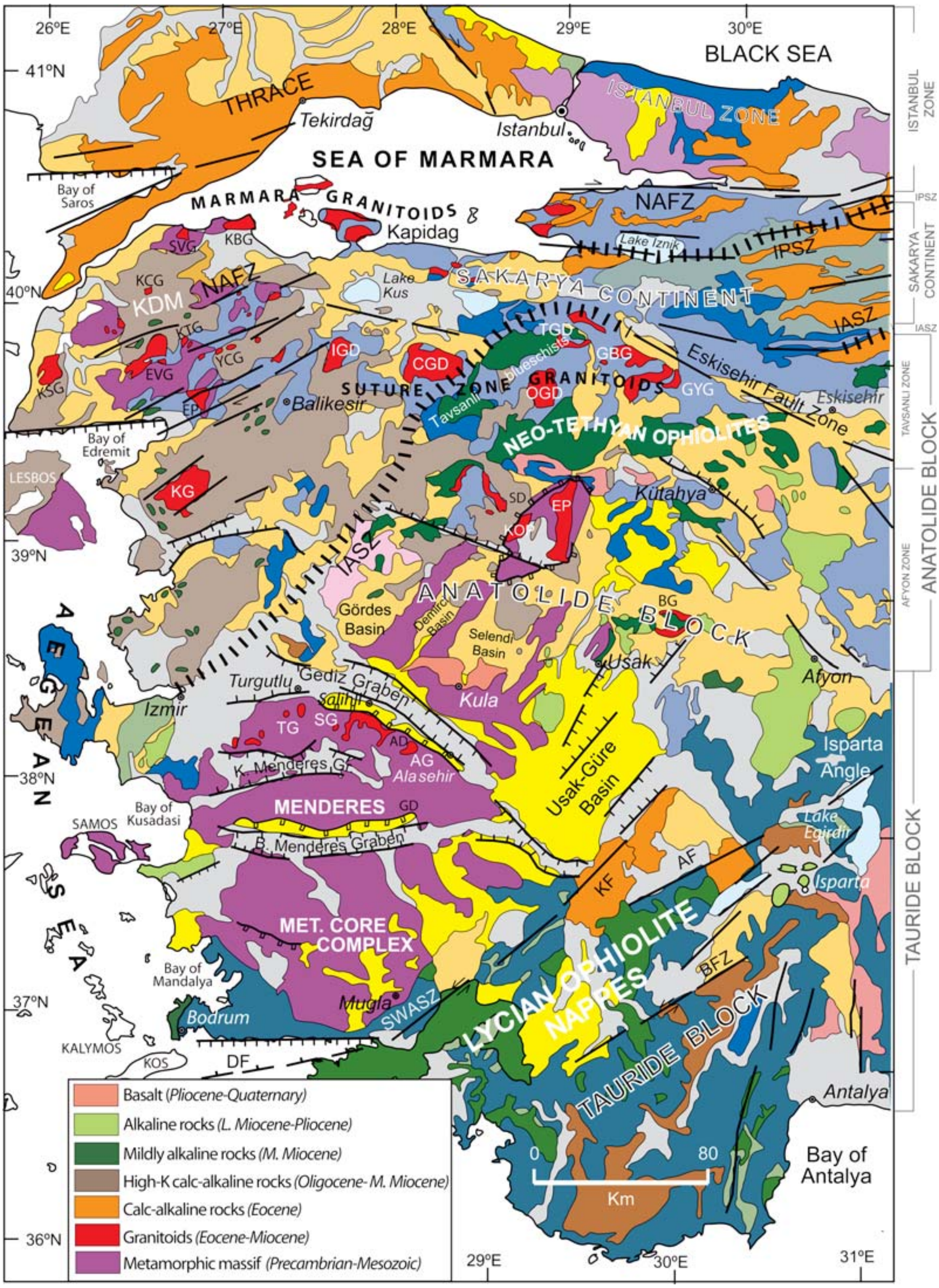

Fig. 7. *Continued.*

intruded by a series of east–west trending Eocene and Oligo–Miocene granitoid plutons (Fig. 7; Bingöl *et al.* 1982, 1994; Delaloye & Bingöl 2000; Altunkaynak 2007). The Kazdag massif within the western part of the Sakarya continent (KDM in Fig. 7) represents a metamorphic core complex, which is inferred to have been exhumed from a depth of *c*. 14 km along a north-dipping mylonitic shear zone starting at *c*. 24 Ma (Okay & Satir 2000).

Izmir–Ankara Suture Zone (IASZ) and Tethyan Ophiolites

The Izmir–Ankara Suture Zone south of the Sakarya continent includes dismembered Tethyan ophiolites, high-pressure low-temperature (HP–LT) blueschist-bearing rocks, and flysch deposits mainly occurring in south-directed thrust sheets (Fig. 7; Önen & Hall 1993; Okay *et al.* 1998; Sherlock *et al.* 1999). Late-stage diabasic dykes crosscutting the ophiolitic units in the Kütahya area are dated at *c*. 92–90 Ma ($^{40}Ar/^{39}Ar$ hornblende ages; Önen 2003), indicating a minimum late Cretaceous igneous age for the ophiolites. The blueschist rocks along the suture zone in the Tavsanli area have yielded $^{40}Ar/^{39}Ar$ cooling ages (phengite crystallization during exhumation) of 79.7 ± 1.6–82.8 ± 1.7 Ma (Sherlock *et al.* 1999), suggesting a latest Cretaceous age for the HP–LT metamorphism in the region. The Lycian nappes and ophiolites that occur farther south in the Tauride block (Fig. 7; Collins & Robertson 2003; Ring & Layer 2003; Çelik & Chiaradia 2008) represent the tectonic outliers of the Cretaceous oceanic crust derived from the IASZ. The Lycian nappes are inferred to have once covered the entire Anatolide belt in western Anatolia, and to have been later removed as a result of tectonic uplift and erosion associated with exhumation of the Menderes core complex during the late Cenozoic (Ring & Layer 2003; Thomson & Ring 2006; Dilek & Altunkaynak 2007).

Menderes massif

The Menderes massif represents a core complex composed of high-grade metamorphic rocks of Pan-African affinity that are intruded by synkinematic Miocene granitoid plutons (Hetzel & Reischmann 1996; Bozkurt & Satir 2000; Bozkurt 2004; Gessner *et al.* 2004). Rimmelé *et al.* (2003) estimated the *P–T* conditions of the metamorphic peak for the Menderes massif rocks at >10 kbar and >440 °C. The main episode of metamorphism is inferred to have resulted from the burial regime associated with the emplacement of the Lycian nappes and ophiolitic thrust sheets (Yilmaz 2002). Imbricate stacking of the Menderes massif beneath the Lycian nappes and ophiolitic thrust sheets appears to have migrated southwards throughout the Palaeocene–Middle Eocene (Özer *et al.* 2001; Candan *et al.* 2005). Unroofing and exhumation of the Menderes massif may have started as early as the Oligocene (25–21 Ma) based on the cooling ages of syn-extensional granitoid intrusions that crosscut the metamorphic rocks (Bozkurt & Satir 2000; Catlos & Çemen 2005; Ring & Collins 2005; Thomson & Ring 2006). This timing may signal the onset of post-collisional tectonic extension in the Aegean region.

Tauride Block in Western Anatolia

The Tauride Block south of the Menderes core complex consists of Precambrian and Cambro–Ordovician to lower Cretaceous carbonate rocks intercalated with volcano-sedimentary and epiclastic rocks (Ricou *et al.* 1975; Demirtasli *et al.* 1984; Özgül 1984; Gürsu *et al.* 2004). These rocks are tectonically overlain by Tethyan ophiolites (i.e. Lycian, Beysehir, Alihoca and Aladag ophiolites) along south-directed thrust sheets (Dilek *et al.* 1999*a*; Collins & Robertson 2003; Çelik & Chiaradia 2008; Elitok & Drüppel 2008). Underthrusting of the Tauride carbonate platform beneath the Tethyan oceanic crust and its partial subduction at a north-dipping subduction zone in the Inner-Tauride Ocean resulted in HP–LT metamorphism (Dilek & Whitney 1997; Okay *et al.* 1998). Continued convergence caused crustal imbrication and thickening within the platform and resulted in the development of several major overthrusts throughout the Tauride block (Demirtasli *et al.* 1984; Dilek *et al.* 1999*b*).

Tectonic evolution of the western Anatolian orogenic belt

Emplacement of the Cretaceous ophiolites onto the Anatolide–Tauride block along the Izmir–Ankara suture zone and partial subduction of the continental edge that led to its HP–LT metamorphism (Sherlock *et al.* 1999; Okay 2002; Ring & Layer 2003; Ring *et al.* 2003) in the late Cretaceous mark the initial stages of collision tectonics in western Anatolia (Fig. 8). The terminal closure of the Northern Tethyan seaway resulted in the collision of the Sakarya continent with the Anatolide–Tauride block during the early Eocene that, in turn, caused regional deformation, metamorphism and crustal thickening. This Barrovian-type, collision-driven regional metamorphism was responsible for the development of high-grade rocks in the Kazdag and Menderes metamorphic

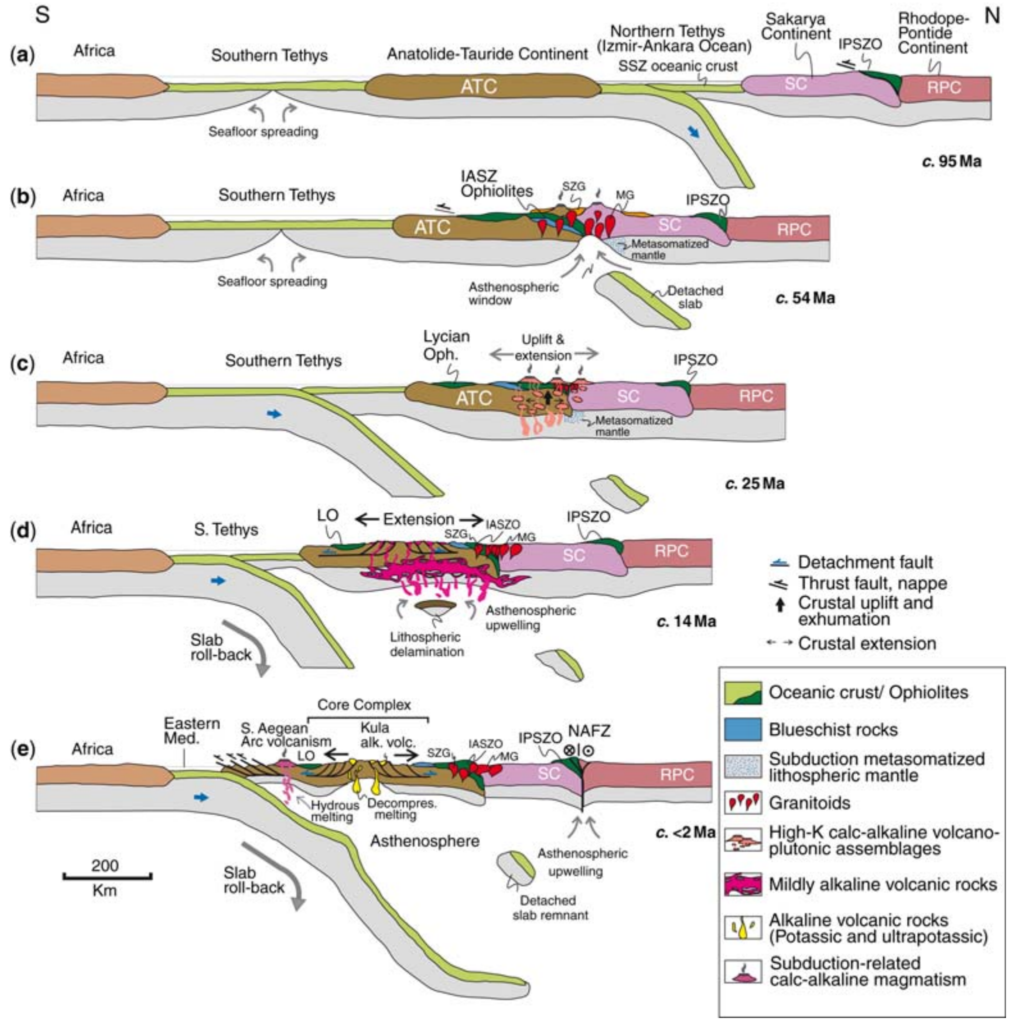

Fig. 8. Late Mesozoic–Cenozoic geodynamic evolution of the western Anatolian orogenic belt as a result of collisional and extensional processes in the upper plate of north-dipping subduction zone(s) within the Tethyan realm. See text for discussion.

massifs. Resistance of the buoyant Anatolide–Tauride continental crust to subduction and consequent arrest of the north-dipping subduction zone resulted in isostatic uplift of its partially subducted passive margin, exhumation of high-P rocks, and rapid denudation of upper crustal rocks, leading to widespread flysch formation during the early to middle Eocene (Ring *et al.* 2003, and references therein).

With continued continental collision the leading edge of the subducted Tethyan slab possibly broke off from the rest of the continental lithosphere, resulting in the development of an asthenospheric window (Fig. 8). Slab detachment and breakoff is a natural response to the gravitational settling of subducted lithosphere in continental collision zones, as a result of a decrease in the subduction rate caused by the positive buoyancy of partially subducted continental lithosphere (Davies & von Blackenburg 1995; von Blackenburg & Davies 1995; Wortel & Spakman 2000; Gerya *et al.* 2004). Our seismic tomography model (Fig. 4) shows the existence of a second high-velocity (cold) slab near the 660 km discontinuity in the lower mantle north of the Hellenic slab, which we interpret as a detached Tethyan slab dipping beneath the western Anatolian orogenic belt. This implies a punctuated evolution of Tethyan subduction zones in the eastern Mediterranean, rather than the single subduction zone hypothesized for much of the Mesozoic and the entire Cenozoic in some recent geodynamic models (i.e. van Hinsbergen *et al.* 2005; Jolivet & Brun 2008).

As the downgoing oceanic plate breaks off, the asthenosphere rises rapidly and is juxtaposed against the thickened mantle lithosphere in the collision zone (Fig. 8, *c.* 54 Ma). Conductive heating of this overriding lithosphere results in melting of the metasomatized and hydrated layers, producing potassic, calc-alkaline magmas. Crustal melting at shallow depths, induced by asthenospheric upwelling, causes granitic/rhyolitic magmatism. Hence, the middle to late Eocene emplacement of widespread granitoid plutons in northwestern Anatolia, mainly through the IASZ and the Sakarya continent (Orhaneli, Topuk, Göynükbelen, etc.), is thought to be a direct result of the heat flux through this window and the associated thermal perturbation that caused melting of the metasomatized continental lithospheric mantle (Dilek & Altunkaynak 2007). Major and trace element compositions of I-type granitoid rocks in NW Anatolia, dated at *c.* 54–35 Ma ($^{40}Ar/^{39}Ar$ hornblende and mica separates, and SHRIMP zircon dating; Dilek & Altunkaynak, unpublished data) indicate their origin by melting of a subduction-modified mantle source that had been enriched in mobile incompatible elements (Altunkaynak 2004, 2007; Köprübasi & Aldanmaz 2004), a signature that is consistent with post-collisional magmatism driven by slab breakoff in other orogenic belts (Schliestedt *et al.* 1987; Hansmann & Oberli 1991; Davies & von Blackenburg 1995; Nemcok *et al.* 1998).

Geological evidence in support of the inferred slab breakoff magmatism in western Anatolia includes: (1) the linear distribution of the plutons in a narrow belt straddling the IASZ where ophiolitic and high-P blueschist rocks are exposed (Figs 7 & 8) – a pattern that suggests a focused heat source likely derived from an asthenospheric window; and (2) the attempted subduction of Anatolide–Tauride continental crust to a depth of $\geq$80 km (Okay *et al.* 1998), evidenced by the latest Cretaceous blueschist rocks of the Tavsanli zone, that is likely to have clogged the subduction zone and caused the detachment of the sinking Tethyan oceanic lithosphere.

Continued collision of the Sakarya and Anatolide–Tauride continental blocks led to the development of thick orogenic crust, orogen-wide burial metamorphism, and anatectic melting of the lower crust (*c.* 25 Ma, Fig. 8). This episode of post-collisional magmatism coincided with bimodal volcanism and a widespread ignimbrite flare-up in western Anatolia (Ercan *et al.* 1985; Yilmaz *et al.* 2001), and caused thermal weakening of the crust in the western Anatolian orogenic belt that led to its extensional collapse. The Kazdag core complex in NW Anatolia (Figs 7 & 8) began its initial exhumation in the latest Oligocene–Early Miocene (Okay & Satir 2000) and the Menderes core complex in central western Anatolia (Fig. 7) underwent its exhumation in the earliest Miocene (Isik *et al.* 2004; Thomson & Ring 2006; Bozkurt 2007). Some of the collision-generated thrust faults may have been reactivated during this time as crustal-scale low-angle detachment faults (e.g. Simav detachment fault, SW Anatolian shear zone), facilitating regional extension (Thomson & Ring 2006; Çemen *et al.* 2006).

Starting in the middle Miocene, both lithospheric and asthenospheric mantle melts were involved in the evolution of bimodal volcanic rocks in western Anatolia with the lithospheric input diminishing in time (Akay & Erdogan 2004; Aldanmaz *et al.* 2000, 2006). The timing of this magmatism coincides with widespread lower crustal exhumation and tectonic extension across the Aegean region (*c.* 14 Ma in Fig. 8). This extensional phase and the attendant mildly alkaline volcanism are attributed to thermal relaxation associated with possible delamination of the subcontinental lithospheric mantle beneath the northwestern Anatolian orogenic belt (Altunkaynak & Dilek 2006; Dilek & Altunkaynak 2007, and references therein). Lithospheric delamination may have been triggered by peeling of the base of the subcontinental lithosphere as a result of slab roll-back at the Hellenic trench.

During the advanced stages of extensional tectonism in the late Miocene–Quaternary, the development of regional graben systems (i.e. Gediz, Büyük Menderes, Fig. 7) further attenuated the continental lithosphere beneath the region. This extensional phase was accompanied by upwelling of the asthenospheric mantle and consequent decompressional melting (Fig. 8). Lithospheric-scale extensional fault systems acted as natural conduits for the transport of uncontaminated alkaline magmas to the surface (Richardson-Bunbury 1996; Seyitoglu *et al.* 1997; Alici *et al.* 2002). Asthenospheric flow in the region following the late Miocene ($<$10 Ma) may also have been driven in part by the extrusion tectonics caused by the Arabian collision in the east, as suggested by the parallelism of the SW-oriented shear wave splitting fast polarization direction in the mantle with the motion of the Anatolian plate (Sandvol *et al.* 2003*b*; Russo *et al.* 2001). This SW-directed lower mantle flow beneath Anatolia could have played a significant role in triggering intra-plate deformation via extension and strike-slip faulting parallel to the flow direction and horizontal mantle thermal anomalies, which would have facilitated melting and associated basaltic volcanism. This lateral asthenospheric flow may also have resulted in the interaction of different compositional end-members, contributing to the mantle heterogeneity beneath western Anatolia. Lateral displacement of the asthenosphere as a result of the extrusion of collision-entrapped ductile mantle beneath Asia and SE Asia has been similarly identified as the cause of post-collisional high-K volcanism in Tibet and Indo–China during the late Cenozoic (Liu *et al.* 2004; Williams *et al.* 2004; Mo *et al.* 2006).

The apparent SW propagation of Cenozoic tectonic extension and magmatism through time is likely to have been the combined result of slab rollback associated with the subduction of the Southern Tethys ocean floor at the Hellenic trench and the thermally induced collapse of the western Anatolian orogenic belt (Fig. 8). The thermal input and melt sources were likely provided first by slab breakoff-generated asthenospheric flow, then by lithospheric delamination-related asthenospheric flow and finally by tectonic extension-driven upward asthenospheric flow and collision-induced (Arabia-Eurasia collision) lateral (westward) mantle flow (Innocenti *et al.* 2005; Dilek & Altunkaynak 2007). Since the late Miocene, subduction zone magmatism related to the retreating Hellenic trench has been responsible for the progressive southward migration of the South Aegean Arc (Fig. 8; Pe-Piper & Piper 2006). The exhumation of high-P rocks in the Cyclades was likely driven by upper plate extension and channel flow associated with this subduction (Jolivet *et al.* 2003; Ring & Layer 2003).

Regional geology of central Anatolia

Much of central Anatolia is occupied by the Central Anatolian Crystalline Complex (CACC), which consists of the Kirsehir, Akdag and Nigde metamorphic massifs, dismembered Tethyan ophiolites, and felsic to mafic plutons ranging in age from the late Cretaceous to the Miocene (Fig. 9; Güleç 1994; Boztug 2000; Düzgören-Aydin 2000; Kadioglu *et al.* 2003, 2006; Ilbeyli 2004; Ilbeyli *et al.* 2004). Several curvilinear sedimentary basins (Tuzgölü, Ulukisla and Sivas), which initially evolved as peripheral foreland and/or forearc basins in the late Cretaceous, delimit the CACC in the west, the east and the south. The south–central part of the CACC includes the Cappadocian volcanic province, containing Upper Miocene to Quaternary volcanic-volcaniclastic rocks and polygenetic volcanic centers (Toprak *et al.* 1994; Dilek *et al.* 1999*b*).

Metamorphic massifs

Protoliths of the high-grade rocks in the metamorphic massifs of the CACC were Palaeozoic to Mesozoic pelitic sediments with local mafic lava units and hypabyssal rocks (Dilek & Whitney 2000, and references therein). These sedimentary units underwent regional metamorphism as a result of burial beneath the Tethyan ophiolites derived from the Izmir–Ankara–Erzincan suture zone to the north (Seymen 1984; Göncüoglu *et al.* 1991; Whitney & Dilek 1998). Subsequent collisional events in the latest Mesozoic and early Cenozoic resulted in further crustal imbrication and thickening of crystalline rocks in the CACC (Dilek *et al.* 1999*b*). Three main massifs (Kirsehir, Akdag and Nigde; Fig. 9) have been delineated in the CACC based on different P–T–t paths of their protoliths.

The Kirsehir massif in the NW part of the CACC consists of marble and calcsilicate rocks interlayered with metapelitic/psammitic schist, amphibolite ($\pm$ garnet), and quartzite (Whitney *et al.* 2001). The metamorphic grade appears to increase from 450 °C (garnet zone) in the SE to *c.* 750 °C (sillimanite zone) in the NW within the massif. The pressure corresponding to peak temperatures for the garnet zone rocks is estimated to be 2.5–4 kbar based on the structural position of these rocks (Whitney *et al.* 2001). However, pressures of *c.* 6 kbar are estimated from the first appearance of garnet in amphibolite-facies rocks in the NW part of the massif.

The Akdag massif represents the largest coherent block of metamorphic rocks in the NE part of the CACC (Fig. 9), metamorphic grade of which ranges from chlorite zone to sillimanite–K-feldspar zone. The highest grade rocks occur in an elongate NE–SW-trending belt along the central axis of the Akdag massif (Whitney *et al.* 2001) containing abundant garnet–muscovite–quartz gneiss (Whitney *et al.* 2001). Various thermometry and barometry applications using different equilibrium phase assemblages in the Akdag metamorphic rocks have revealed peak pressures ranging from 5 ± 1–8 ± 1 kbar and peak temperatures ranging from 550–600 to 660–675 °C (Whitney *et al.* 2001).

The Nigde massif in the southern part of the CACC (Fig. 9) is exposed in a structural dome that has been interpreted as a Cordilleran-type metamorphic core complex (Whitney & Dilek 1997). A gently (*c.* 30°) S-dipping detachment fault bounding the Nigde massif along its southern edge juxtaposes multiply deformed marble, quartzite and schist in the footwall from clastic sedimentary rocks of the Ulukisla basin in the hanging wall. The central part of the Nigde massif consists predominantly of upper amphibolite facies metasedimentary rocks and the peraluminous Uçkapili granite. These metapelitic rocks record an earlier episode of regional, medium-pressure/high temperature metamorphism (5–6 kbar and T > 700 °C), and a younger episode of low-pressure/high temperature metamorphism (730–770 °C) (Whitney & Dilek 1998; Fayon *et al.* 2001). The earlier event was most likely

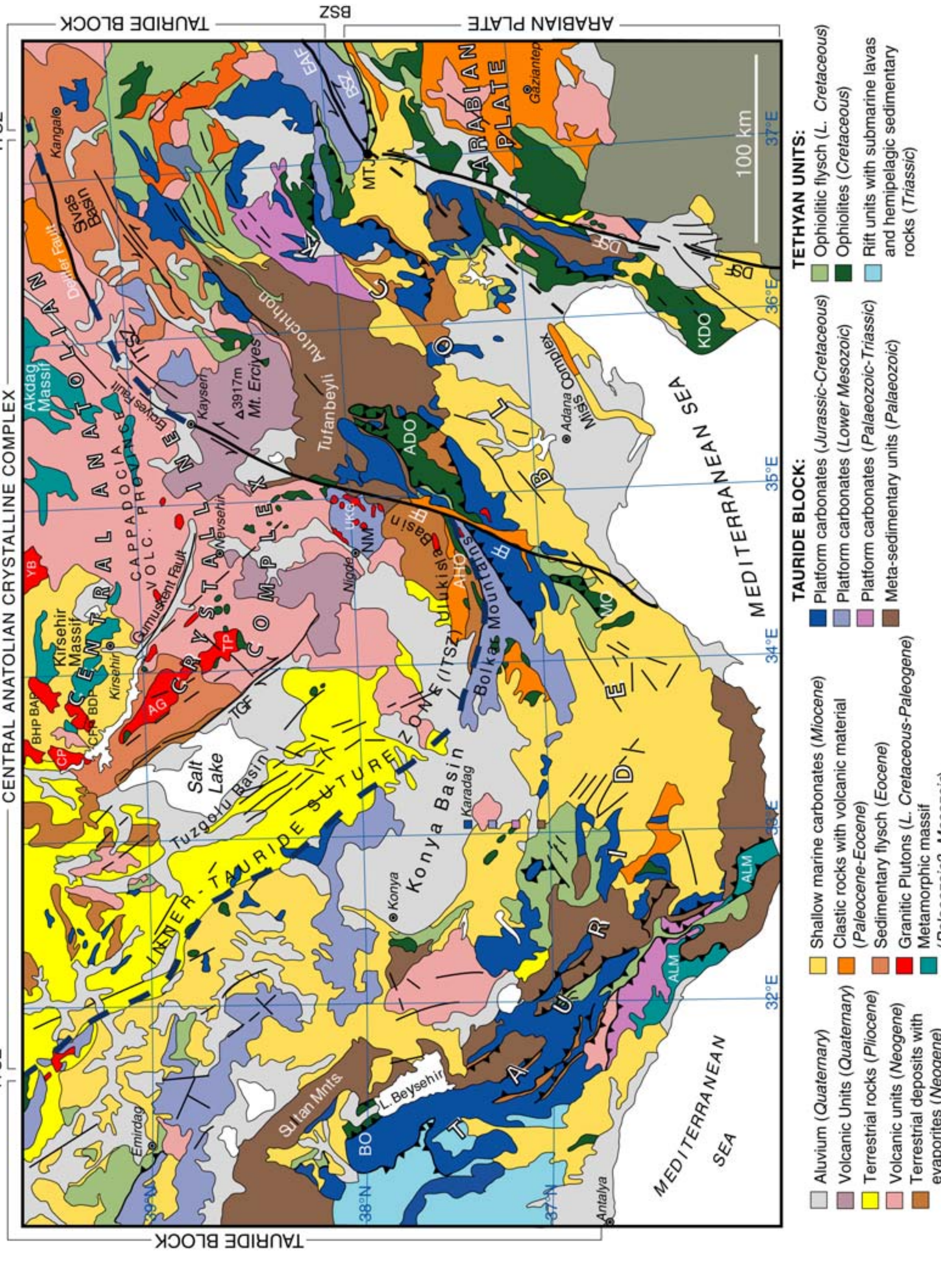

Fig. 9. *Continued.*

related to burial and heating after emplacement of the Tethyan ophiolites southward onto the CACC during the late Cretaceous and during the subsequent collision between the CACC and Tauride blocks, whereas the younger event was associated with shallow intrusion of the Uçkapili granite, which crosscuts the metamorphic and structural fabrics in the Nigde massif.

The P–T–t paths of the Akdag and Kirsehir massifs indicate that the northern part of the CACC where they are now exposed was deformed, metamorphosed and unroofed during tectonic events associated with the collision of the CACC with a south-facing intraoceanic arc in the northern branch of the Tethys, followed by a collision with the Pontide arc to the north in the early to mid-Eocene. The sedimentary rocks of the Akdag and Kirsehir massifs were buried to moderate depths (*c*. 20 km) beneath the Tethyan ophiolite nappes derived from the Izmir–Ankara–Erzincan suture zone and were thickened via folding and thrust faulting. The existence of kyanite in the Akdag massif rocks suggests that the eastern part of the CACC either experienced greater degrees of crustal thickening or was exhumed from deeper crustal levels than the rest of the massifs in the CACC. The northern part of the CACC was slowly exhumed via erosion by the Eocene (Fayon *et al.* 2001).

The SW part of the CACC experienced relatively high-temperature metamorphism associated with extensive Andean-type arc magmatism at relatively shallow crustal levels that are represented by the CACC plutons (see below). The southern part of the CACC, where the Nigde massif is now exposed, experienced Barrovian metamorphism at mid-crustal pressures (*c*. 5–6 kbar) and at high temperatures (>700 °C), possibly associated with orogenic crustal thickening (Whitney & Dilek 1998). The Nigde core complex was exhumed to <2 km depth mainly by tectonic unroofing along low-angle detachment faults. Apatite fission track ages from the Nigde rocks range from *c*. 9–12 Ma and indicate slow to moderate cooling via exhumation at rates of 30–8 °C/Ma (Fayon *et al.* 2001). Thus, different unroofing mechanisms appear to have affected the CACC since the early Oligocene: the northern CACC undergoing erosional unroofing nearly 20 Ma before the tectonic exhumation of the southern CACC starting in the late Miocene.

Inner-Tauride suture zone (ITSZ) and Tethyan ophiolites

Discontinuous exposures of the Tethyan ophiolites and mélanges define two major suture zones surrounding the CACC in the north and the south. The Izmir–Ankara–Erzincan suture zone to the north and the Inner-Tauride suture (ITSZ) zone to the south (Fig. 1b) mark the obliteration sites of the Tethyan seaways, which had evolved between the Gondwana-derived continental fragments (Sengör & Yilmaz 1981; Robertson & Dixon 1984; Dilek & Moores 1990). Subduction of the Tethyan oceanic lithosphere that evolved in these seaways resulted in the development of incipient arc-forearc complexes that subsequently formed the ophiolites, in the mantle heterogeneity beneath the continental fragments, and eventually, in continental collisions in the Eocene (Dilek & Flower 2003).

Ophiolite complexes within the Izmir–Ankara–Erzincan suture zone include serpentinized upper mantle peridotites and gabbros that are crosscut by dolerite and plagiogranite dikes and overlain by pillow lavas (Tankut *et al.* 1998; Dilek & Thy 2006). Both dolerite and plagiogranite dykes show negative Ta–Nb patterns typical of arc-related petrogenesis and zircon ages of *c*. 179 ± 15 Ma, indicating that the ophiolitic basement in the Izmir–Ankara–Erzincan suture zone is at least early Jurassic in age or older (Dilek & Thy 2006). The Inner-Tauride ophiolites to the south (i.e. Alihoca, Aladag, Mersin) consist mainly of tectonized harzburgites, mafic-ultramafic cumulates and gabbros, and commonly lack sheeted dykes and extrusive rocks (Parlak *et al.* 1996, 2002; Dilek *et al.* 1999*a*). They include thin (*c*. 200 m) thrust sheets of metamorphic sole rocks beneath them, and both the ophiolitic units and the sole rocks are intruded by mafic dyke swarms composed of basaltic to andesitic rocks with island arc tholeiite (IAT)

Fig. 9. Geological map of the central Anatolian region, showing the distribution of Tethyan ophiolites, suture zones, major tectonostratigraphic units within the Tauride block and the Central Anatolian Crystalline Complex (CACC) (including metamorphic massifs and major plutons), and major faults systems. Key to lettering of major granitoid plutons in the CACC: AG, Agaçören granitoid; BAP, Bayindir pluton; BDP, Baranadag pluton; BHP, Behrek Dag pluton; CFP, Cefalik pluton; CP, Çelebi pluton; TP, Terlemez pluton; UKG, Uçkapili granite; YB, Yozgat batholith. Key to lettering of major fault systems: BSZ, Bitlis suture zone; DSF, Dead Sea Fault; EAF, East Anatolian Fault; EF, Ecemis Fault; ITSZ, Inner-Tauride Suture Zone; TGF, Tuzgölü Fault. Major ophiolites: ADO, Aladag ophiolite; AHO, Alihoca ophiolite; BO, Beysehir ophiolite; KDO, Kizildag ophiolite; MO, Mersin ophiolite. Other symbols: ALM, Alanya massif; MTJ, Maras Triple Junction; NM, Nigde massif; (data are from Dilek & Moores 1990; Dilek *et al.* 1999*a*, *b*; Kadioglu *et al.* 2003, 2006). Notice that the ITSZ, marked by a dark-blue, dashed thick line, is truncated and offset by the sinistral Ecemis fault (EF).

affinities. $^{40}Ar/^{39}Ar$ hornblende ages of 92–90 and 90–91 Ma from the metamorphic sole and dyke rocks, respectively, indicate Cenomanian–Turonian ages for the Inner-Tauride ophiolites (Dilek *et al.* 1999*a*; Parlak & Delaloye 1999; Çelik *et al.* 2006). These age brackets suggest that the Tethyan ophiolites rooted in the Inner-Tauride suture zone are possibly younger than those derived from the Izmir–Ankara–Erzincan suture zone farther north.

In addition to the Cenomanian–Turonian ophiolites, the ITSZ is also marked by discontinuous exposures of blueschist-bearing mafic-ultramafic and carbonate rocks along the northern edge of the Tauride block. The occurrence of sodic amphibole-containing metasedimentary and metavolcanic rocks in the Bolkar Mountains region (Blumenthal 1956; van der Kaaden 1966; Gianelli *et al.* 1972; Dilek & Whitney 1997) extends into the Tavsanli zone in NW Anatolia and into the Pinarbasi zone in the Eastern Taurides in East–Central Anatolia. These HP/LT rock assemblages showing counterclockwise P–T–t trajectories of their metamorphic evolution indicate increasing P/T ratio with cooling that was associated with continuous subduction within the Inner-Tauride Ocean (Dilek & Whitney 1997, 2000). Late Cretaceous–Palaeocene calc-alkaline plutonic rocks (Dilek, unpublished data) intruding into the Ulukisla basin strata north of the Bolkar Mountains point out that this subduction activity had continued into the early Cenozoic.

Syn-collisional CACC plutons

The late Cretaceous plutonic rocks in the CACC were emplaced after obduction of the Cretaceous Tethyan ophiolites, which were derived from the Izmir–Ankara–Erzincan suture zone to the north, and before its collision with the Pontide and Tauride continental blocks during the middle Eocene. Therefore, the magmatic evolution of these plutons preceded the terminal continental collisions in the region (Akiman *et al.* 1993; Erler & Bayhan 1995; Kadioglu *et al.* 2006).

The CACC plutons can be grouped into three supersuites based on their field occurrences and distinct differences in their mineral and chemical compositions (Kadioglu *et al.* 2006). Plutonic rocks of the Granite Supersuite commonly occur in a curvilinear belt along the western edge of the CACC (east of the Salt Lake-Tuzgölü, Fig. 9) and consist of calc-alkaline rocks ranging in composition from tonalite, granodiorite and biotite granite to amphibole biotite granite and biotite-alkali feldspar granite. Plutons of the Monzonite Supersuite (i.e. Terlemez, Cefalik, Baranadag plutons) occur immediately east of the Granite Supersuite plutons and are composed mainly of subalkaline quartz monzonite and monzonite. Both the Granite and Monzonite Supersuite rocks show enrichment in LILE and depletion in HFSE relative to ocean ridge granites (ORG). They display isotopic and trace element signatures suggesting a crustal component that reflect subduction-influenced source enrichment and crustal contamination resulting from assimilation fractional crystallization (AFC) processes during magma transport through the CACC crust (Bayhan 1987; Aydin *et al.* 1998; Güleç & Kadioglu 1998; Kadioglu *et al.* 2003, 2006). There is a progression from high-K calc-alkaline and high-K shoshonitic compositions in the Granite Supersuite to typical shoshonitic compositions in the Monzonite Supersuite rocks.

The Syenite Supersuite represents the youngest phase of plutonism in the late Cretaceous (*c.* 69 Ma) and generally occurs in the inner part of the CACC. Rocks of this supersuite are composed of silica saturated (quartz syenite and syenite) and silica under-saturated, nepheline and pseudoleucite bearing alkaline rocks, which show more enrichment in LILE and a slight enrichment in HFSE in comparison to the other two supersuites (Boztug *et al.* 1997; Kadioglu *et al.* 2006). Isotopic and trace element signatures of the Syenite Supersuite plutons suggest that their magmas were more enriched in within-plate mantle components compared to the Granite and Monzonite Supersuite plutons (Kadioglu *et al.* 2006). $^{40}Ar/^{39}Ar$ age data from these Granite, Monzonite and Syenite Supersuite plutons yield ages of 77.7 ± 0.3, 70 ± 1.0, and 69.8 ± 0.3 Ma, respectively (Kadioglu *et al.* 2006). Thus, the subduction zone influence on melt evolution beneath the CACC appears to have decreased rapidly (within *c.* 7–8 Ma) from the earlier calc-alkaline granitic magmatism to the later alkaline, syenitic magmatism during the latest Cretaceous.

Tauride block

The Tauride block south of the CACC consists of Palaeozoic to upper Cretaceous carbonate, siliciclastic and volcanic rocks (Özgül 1976; Demirtasli *et al.* 1984) and represents a ribbon continent rifted off from the northwestern edge of Gondwana (Robertson & Dixon 1984; Garfunkel 1998). The Palaeozoic–Jurassic tectonostratigraphic units in the Tauride block are tightly folded and imbricated along major thrust faults that developed first during the obduction of the Inner-Tauride ophiolites from the north in the late Cretaceous, and subsequently during the collision of the Tauride block with the CACC in the latest Palaeocene–Eocene. The buoyancy of the Tauride continental crust in the lower plate eventually arrested the subduction process and caused the isostatic rebound of the partially subducted platform edge, leading to block-fault uplifting of the Taurides during the latest Cenozoic (Dilek & Whitney 1997, 2000). The entire Tauride block experienced gradual uplift in the footwall of a north-dipping frontal normal fault system along its northern edge starting in the Miocene, and developed as a southward-tilted, asymmetric mega-fault block with a rugged, alpine topography (Dilek *et al.* 1999*b*). Apatite fission track ages of 23.6 ± 1.2 Ma from the 55 Ma-old Horoz granite that is intrusive into the Bolkar carbonates are consistent with this uplift history (Dilek *et al.* 1999*b*).

Cappadocian volcanic province

The Cappadocian volcanic province defines a *c.* 300 km-long volcanic belt extending NE–SW across the CACC (Fig. 9). The earliest volcanism in the province started in the mid-Miocene (*c.* 13.5 Ma) and continued into the Quaternary (Pasquaré *et al.* 1988; Ercan *et al.* 1994). The initial volcanic products include 13.5–8.5 Ma andesitic lavas, tuff and ignimbrites in the form of effusive centres and endogeneous domes. This volcanic phase was followed by widespread eruption of ignimbrites, volcanic ash, lapilli and agglomerates between 8.5 and 2.7 Ma (Pasquaré *et al.* 1988; Ercan *et al.* 1994). The most recent phase of volcanism produced central volcanoes oriented parallel to the NE–SW axis of the province, consisting of basaltic andesite, andesite, dacite, rhyodacite and basaltic lavas. Geochemically, these rocks collectively have an A-type granitic melt origin showing post-collisional, within-plate affinities (Innocenti *et al.* 1975; Ercan *et al.* 1994; Toprak *et al.* 1994).

The Cappadocian volcanic province broadly corresponds to a structurally controlled topographic depression filled with Upper Miocene to Pliocene fluvial and lacustrine deposits (Dilek *et al.* 1999*b*). The volcanic edifices appear to have been built at the intersections of major strike-slip fault systems (i.e. Mt. Erciyes volcano) and/or in local graben structures associated with tectonic subsidence and a *c.* NNW–SSE-oriented regional extension during the late Cenozoic (Toprak *et al.* 1994; Dilek *et al.* 1999*b*). These relations indicate that faulting and volcanism in the Cappadocian volcanic province were spatially and temporally associated, and that magma transport and extrusion were in part facilitated by crustal-scale fault systems (Dilek *et al.* 1999*b*).

Tectonic evolution of the central Anatolian orogenic belt

The southward emplacement of the Tethyan suprasubduction zone ophiolites along the northern edge of the CACC around 90–85 Ma was facilitated by a subduction zone dipping northward beneath the Pontides and away from the CACC (Tankut *et al.* 1998; Dilek & Whitney 2000; Floyd *et al.* 2000). This subduction zone could not have had any effect on the mantle dynamics and heterogeneity beneath the CACC or on the evolution of the Late Cretaceous magmatism on and across the CACC (as suggested in Boztug 2000; Ilbeyli *et al.* 2004; Köksal *et al.* 2004; Ilbeyli 2005). Instead, the subduction zone that was involved in the evolution of the CACC magmatism was located to the SW, dipping northeastward beneath the CACC (in present coordinate system) and consuming the oceanic lithosphere of the Inner-Tauride Ocean (Fig. 10a; Erdogan *et al.* 1996; Dilek *et al.* 1999*a*; Kadioglu *et al.* 2003). The inferred chemical modification of the mantle wedge beneath the CACC was associated with this ITSZ.

There are several independent lines of evidence for the existence of this Inner-Tauride basin between the CACC and the Tauride block and the northward dipping subduction zone within this Tethyan seaway. The Cenomanian age suprasubduction zone ophiolites in the Tauride belt were derived from the arc-forearc setting in the Inner-Tauride Ocean and were emplaced southward onto the continental edge of the Tauride block during its collision with an intra-oceanic arc-trench system (Dilek *et al.* 1999*a*; Parlak *et al.* 1996). Partial subduction of the Tauride edge beneath the ophiolite nappes resulted in HP/LT metamorphism of the platform carbonates and in the formation of blueschists (Fig. 10b), which are currently exposed discontinuously along the northern periphery of the Tauride belt (Okay 1984; Okay *et al.* 1996, 1998; Dilek & Whitney 1997; Önen 2003). The calculated P–T conditions of metamorphism and $^{40}Ar/^{39}Ar$ ages of phengites and glaucophanes from blueschist rocks in northwestern Anatolia suggest that this HP/LT metamorphism occurred around 88 Ma (Harris *et al.* 1994; Okay *et al.* 1996).

The older peraluminous granitoid plutons (*c.* 100–85 Ma) along the western edge of the CACC represent a magmatic arc complex that developed above a NE-dipping subduction zone within the Inner-Tauride Ocean (Fig. 10b; Görür *et al.* 1984). During the closure of this basin as a result of the subduction of the Tethyan oceanic lithosphere beneath the western edge of the CACC, the melts derived from the metasomatized upper mantle were injected into the continental crust, causing its partial melting. This led to interaction of mantle- and crustal-derived magmas that involved AFC, mixing and mingling which collectively produced the calc-alkaline granitoid plutons (Fig. 10b, c; Erdogan *et al.* 1996; Kadioglu *et al.* 2003; Ilbeyli *et al.* 2004).

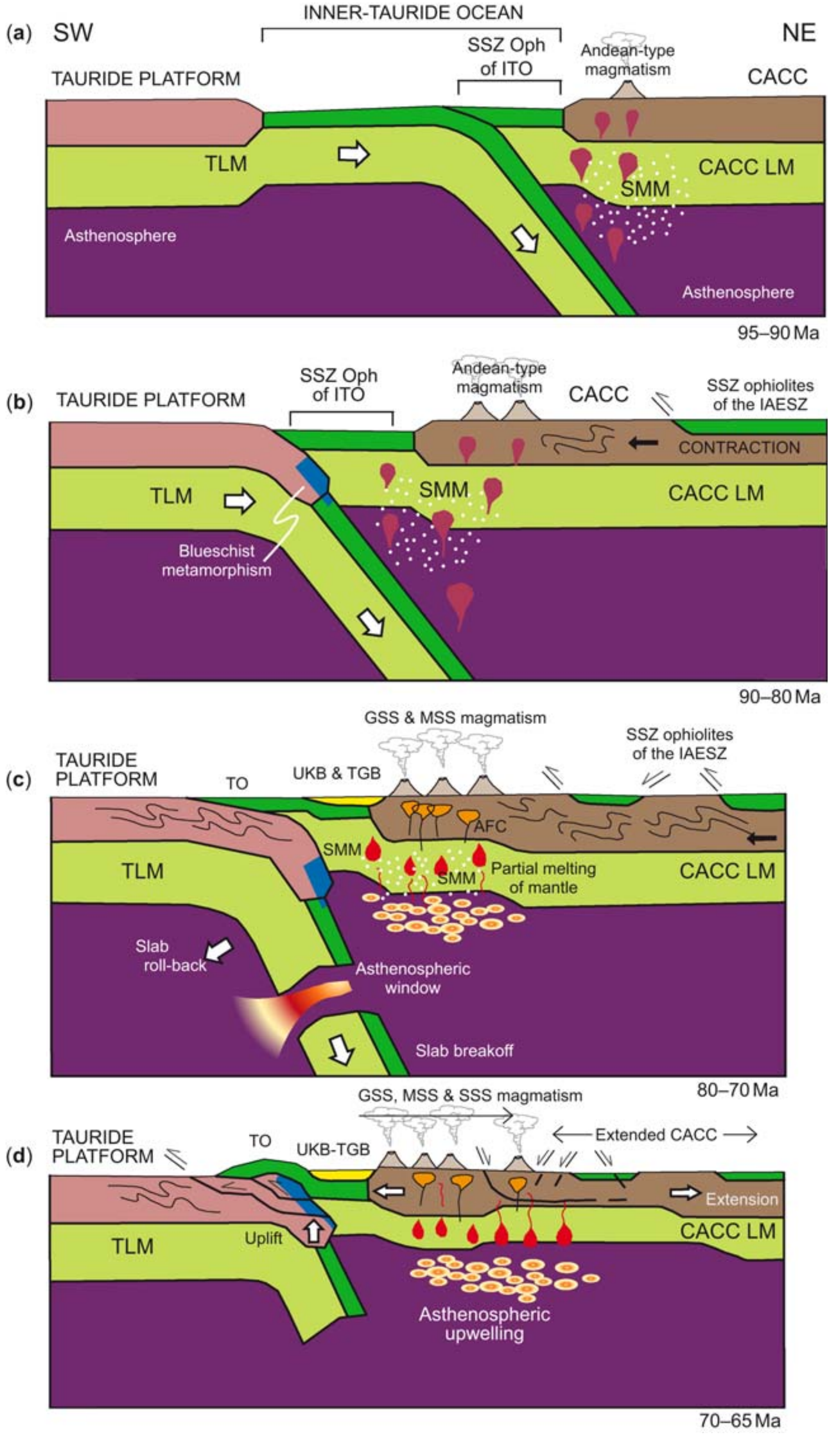

Fig. 10. Tectonic model for the evolution of the CACC and the central Anatolian orogenic belts in the late Mesozoic (modified after Kadioglu *et al.* 2006). See text for discussion. Ellipses beneath SMM depict melting in the asthenosphere. Stippled (in white) pattern characterizes subduction-metasomatized mantle. Key to lettering: AFC, Assimilation

Following the demise of the Inner-Tauride oceanic lithosphere at the NE-dipping subduction zone and the emplacement of the incipient arc-forearc ophiolites onto the northern edge of the Tauride block, subduction was arrested by the underplating of the buoyant Tauride continental crust. The leading edge of the subducted Tethyan slab likely broke off from the rest of the Tauride continental lithosphere, resulting in the development of an asthenospheric window (Fig. 10c). The juxtaposition of this asthenospheric heat source against the overlying continental lithosphere may have caused melting of the metasomatized mantle layers, producing the high-K shoshonitic, adakite-like magmas of the monzonitic plutons and then the more-enriched alkaline magmas of the syenitic plutons (Fig. 10d). This process is similar to that inferred for slab breakoff-related collisional magmatism in other orogenic belts (Davies & von Blackenburg 1995, and references therein) and in the early Cenozoic of western Anatolia, as discussed earlier.

As the asthenosphere moved upwards through the window in the slab, partial melting occurred at the boundary between the lithosphere and asthenosphere producing basaltic melts with transitional characteristics between those of calc-alkaline and alkaline basalts. The mantle sources for these primary basaltic melts may have been metasomatized garnet peridotites and/or spinel lherzolites and phlogopite-bearing lherzolites of an upper mantle wedge origin (Conceiçao & Green 2004). Such slab breakoff-related magmatism with similar calc-alkaline to alkaline products has been documented from other orogenic belts, such as the Neogene–Quaternary Carpathian–Pannonian region (Nemcok *et al.* 1998; Seghedi *et al.* 2004), the Late Palaeogene Periadriatic–Sava–Vardar magmatic zone in the Dinaride–Hellenide mountain belt (Pamic *et al.* 2002), the Neogene Maghrebian orogenic belt in northern Africa (Maury *et al.* 2000) and the late Oligocene–early Miocene central Aegean Sea region (Pe-Piper & Piper 1994).

Thermal perturbation of the continental lithosphere and the alkaline magmatism weakened the orogenic crust, leading to tectonic extension in and across the CACC (Fig. 10d). The results of recent studies of metamorphic massifs and core complexes in central Anatolia suggest that significant crustal extension and unroofing might have occurred within the CACC prior to the Eocene (Gautier *et al.* 2002).

Strike-slip faulting also played a major role in the late Cenozoic tectonic evolution of the CACC. A series of NE–SW and NW–SE trending strike-slip fault systems crosscut both the crystalline basement rocks and the Palaeogene–Quaternary sedimentary strata and volcanic rock units (Fig. 9). The sinistral Ecemis fault (EF) truncates and offsets the Tauride block and the ITSZ by as much as 100 km, and forms mainly a transtensional fault system with several releasing bends and pull-apart structures. It appears to have accommodated top-to-the south extension and crustal exhumation along the south-dipping detachment fault of the Nigde core complex. It may have, therefore, facilitated the vertical displacement and unroofing of high-grade metamorphic rocks in the eastern part of the Nigde massif during the Oligo–Miocene (Dilek & Whitney 1998). The NW–SE trending Tuzgölü fault (TGF) bounding the Cappadocian volcanic province on the west represents a dextral transpressional fault system (Saroglu *et al.* 1992). The latest Cretaceous granitoid plutons and their high-grade metamorphic host rocks in the western part of the CACC have been uplifted on the eastern shoulder of the TGF. The Ecemis and Tuzgölü faults together form a triangular-shaped crustal flake within the CACC that has been moving southwards while undergoing rifting and subsidence, which has given way into the development of the Cappadocian volcanic province throughout the latest Cenozoic.

Regional geology of eastern Anatolia

Much of eastern Turkey is occupied by the East Anatolian High Plateau, which is bounded in the north by the Eastern Pontide arc and in the south by the Bitlis–Pütürge massif (Fig. 11). The mean surface elevation of the plateau is about 2–2.5 km above sea level with scattered Plio–Quaternary volcanic cones over 5 km high (e.g. Mt. Ararat or Mt. Agri). The basement geology of the plateau is composed of ophiolites and ophiolitic mélange, flysch and molasse deposits, and the eastward extension of the Tauride platform carbonates. The Tethyan ophiolites and ophiolitic mélanges, flysch deposits and volcanic arc units collectively constitute the East Anatolian Subduction–Accretion Complex.

Fig. 10. (*Continued*) fractional crystallization; CACC, Central Anatolian Crystalline Complex; CACC LM, Central Anatolian Crystalline Complex lithospheric mantle; IAESZ, Izmir–Ankara–Erzincan suture zone; ITO, Inner Tauride Ocean; SMM, Subduction modified mantle; SSZ, Suprasubduction zone; TGB, Tuzgölü basin; TLM, Tauride lithospheric mantle; TO, Tauride ophiolites (including the Aladag, Alihoca and Mersin ophiolites); UKB, Ulukisla basin. GSS, MSS and SSS magmatism represent the Granite, Monzonite and Syenite Supersuites, respectively, of the syncollisional CACC plutons. SSZ ophiolites of the Inner-Tauride Ocean (ITO) include the Beysehir, Alihoca, Aladag, and Mersin ophiolites.

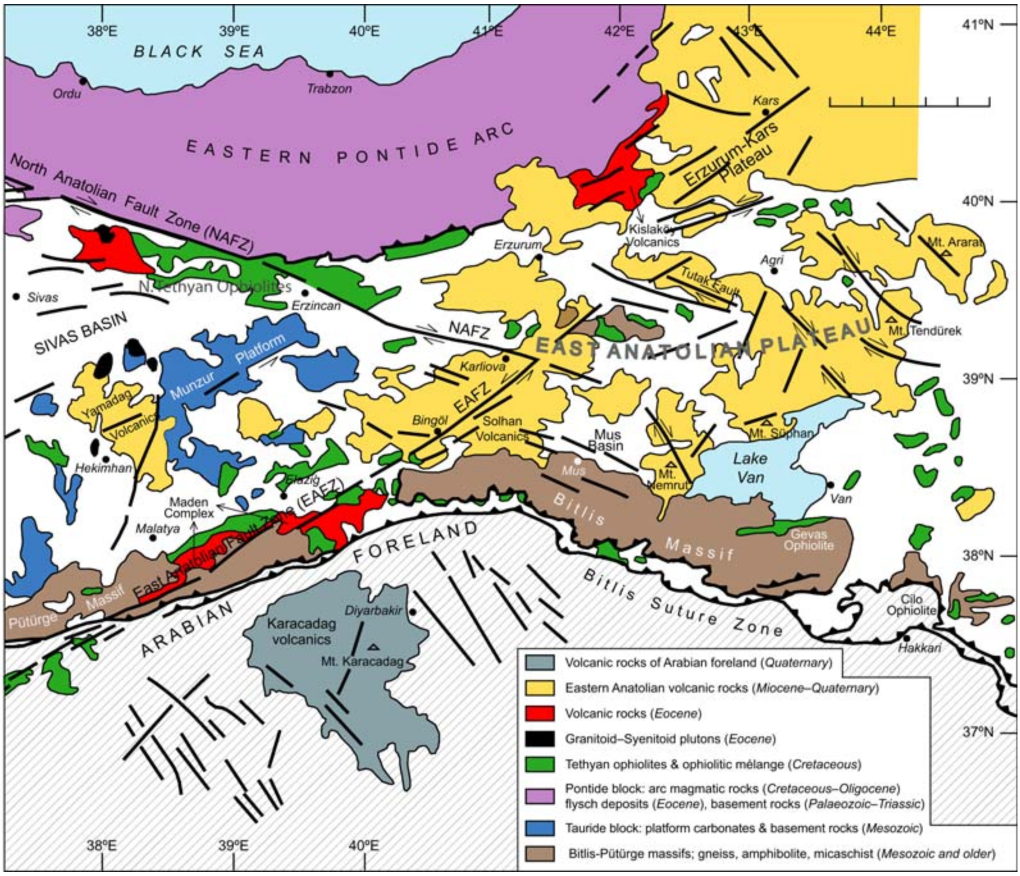

Fig. 11. Simplified geological map of Eastern Anatolia and the Arabian foreland. Munzur Platform constitutes the eastern extension of the platform carbonates and basement rocks of the Tauride block. Bitlis–Pütürge massif is a rifted off fragment of the Arabian plate, analogous to the Tauride block. The East Anatolian Plateau is covered by Miocene–Quaternary volcanic rocks; its basement is composed of Tethyan ophiolites and ophiolitic mélanges, flysch and molasses deposits, and platform carbonates of the Tauride block. Key to lettering: EAFZ, East Anatolian fault zone; NAFZ, North Anatolian fault zone.

Eastern Pontide arc

The Pontide block north of the plateau represents a south-facing early Cretaceous–late Eocene volcano-plutonic arc that developed over a subduction zone dipping northward beneath the Eurasian continental margin (Yilmaz *et al.* 1997). The collision of the Pontide arc with the Tauride microcontinent in the late Eocene terminated the subduction zone magmatism in the Pontide terrane and produced extensive flysch deposits with intense folding in the collision zone (Dewey *et al.* 1986).

Bitlis–Pütürge massif

The Bitlis–Pütürge massif is a nearly East–West-trending microcontinent that is surrounded on all sides by ophiolitic rocks, mélanges, and volcanic and volcaniclastic rocks of an arc origin. The Sanandaj–Sirjan continental block to the SE in Iran represents the eastern continuation of the Bitlis–Pütürge massif in the peri-Arabian region. The Sanandaj–Sirjan continental block to the SE in Iran represents the eastern continuation of the Bitlis–Pütürge massif in the peri-Arabian region. The Pütürge massif is composed of pre-Triassic gneisses and micaschists, and granitoids (Michard *et al.* 1984; Aktas & Robertson 1990) and is interpreted as a pre-Triassic continental sliver of Afro–Arabian origin, similar to the Bitlis massif to the east. The Pütürge massif and the overlying volcanic and ophiolitic rocks are structurally underlain in the south by an upper Cretaceous–early Tertiary mélange, which is underthrust to the south by the foreland sedimentary sequences of the Arabian plate (Fig. 12).

The Bitlis massif is a composite tectonic unit, which is composed of a metamorphic basement

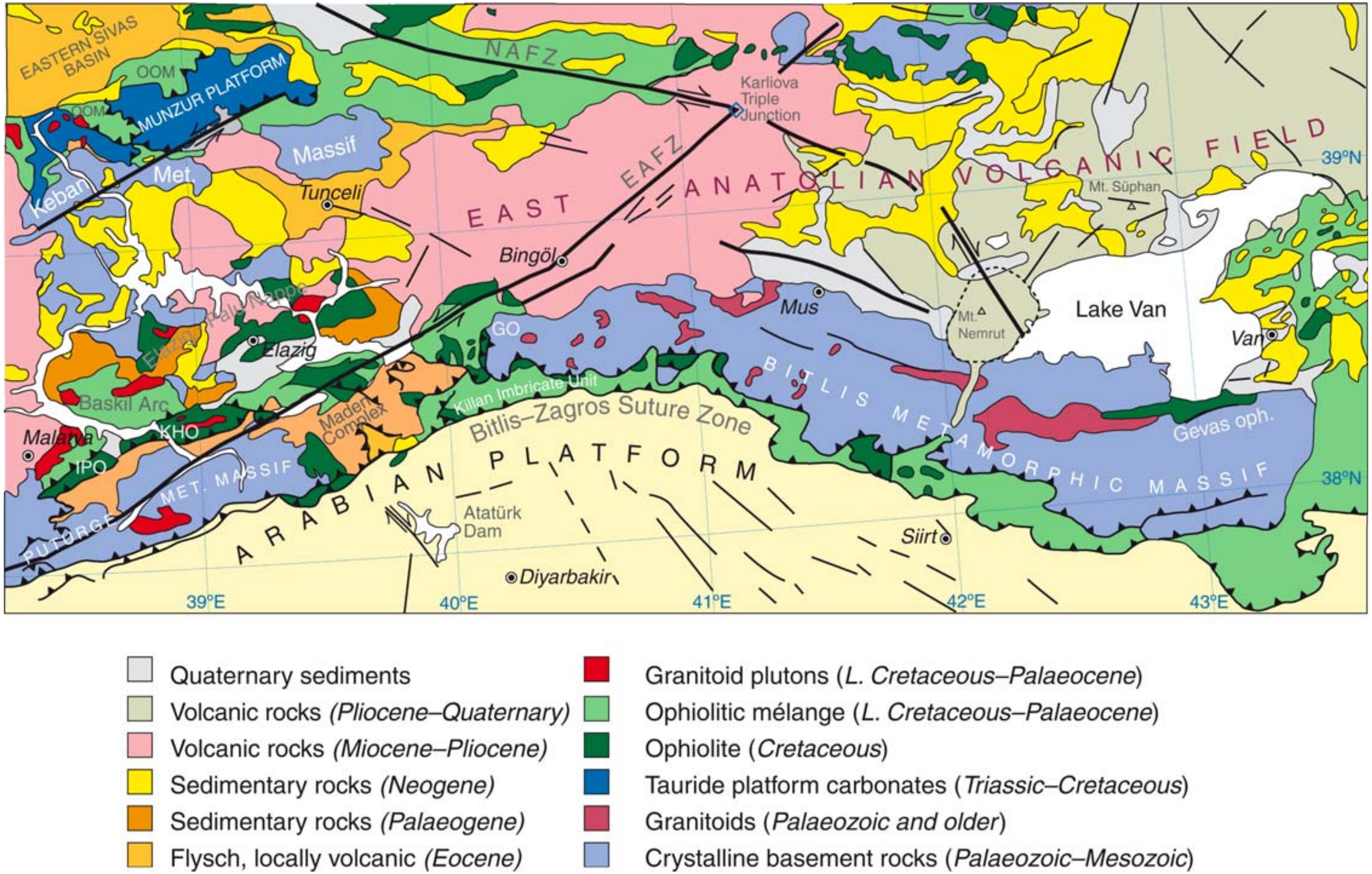

Fig. 12. Simplified tectonic map of Eastern Anatolia showing the basement geology, which consists of metamorphic massifs, ophiolites, ophiolitic mélanges, magmatic arcs, flysch deposits, Tauride platform carbonates, main fault zones, and the distribution of the major Plio–Quaternary volcanic eruptive centres and the Miocene–Pliocene volcanic rocks in the East Anatolian High Plateau. EAFZ and NAFZ mark the East and North Anatolian fault zones, respectively. Symbols for the ophiolites: GO, Guleman; IPO, Ispendere; KHO, Kömürhan; OOM, Ovacik ophiolitic mélange.

(Precambrian?), overlying metamorphosed Palaeozoic to Triassic carbonate rocks (Göncüoglu & Turhan 1984; Helvaci & Griffin 1984), and Palaeozoic to late Mesozoic granitoids (Fig. 12). Oberhänsli *et al.* (2008) recently reported a regionally distributed LT/HP metamorphic overprint in the thermal evolution of the Bitlis massif and suggested that the massif is composed of a stack of nappes formed during the closure of the Southern Tethys between Arabia and the Anatolide–Tauride continental block. The whole massif displays a doubly plunging, multiply folded anticlinorium with overturned limbs both to the north and the south (Dilek & Moores 1990). The relatively youngest thrust faults are south-vergent and synthetic to the Bitlis suture that represents the collision zone between the Arabian and Eurasian plates.

East Anatolian subduction-accretion complex

The Jurassic (?)–Cretaceous ophiolites underlying the molasse deposits and the Tertiary volcanic cover in the western part of the East Anatolian High Plateau represent the remnants of Mesozoic Tethys and are commonly directed southwards onto the margins of the Eastern Tauride platform and the Pütürge massif (Dilek & Moores 1990). The Maastrichtian Ovacik ophiolitic mélange overlies tectonically the Upper Triassic–Cretaceous Munzur platform (Fig. 12) that is interpreted to be the northeastward extension of the calcareous axis of the Tauride block (Özgül & Tursucu 1984). The Ovacik mélange consists of blocks of serpentinites, metamorphic rocks and pelagic limestones in a fine-grained, phyllitic matrix and is unconformably overlain by Maastrichtian clastic rocks (Özgül & Tursucu 1984). Both the Ovacik mélange and Munzur carbonates are thrust to the south over the Keban metamorphic rocks that consist of Permian to Cretaceous metamorphosed platform carbonates (Fig. 12; Michard *et al.* 1984). The Keban metamorphics and Munzur carbonates display north-vergent, upright folds that have been subsequently folded by south-vergent folds (Dilek & Moores 1990).

The Keban metamorphic rocks overlie tectonically the Elazig–Palu nappe to the south along south-vergent thrust faults (Fig. 12). The Elazig–Palu nappe consists of calc-alkaline intrusive and extrusive rocks, and overlying Campanian–Maastrichtian volcaniclastic and flysch deposits (Michard *et al.* 1984; Yazgan 1984; Aktas & Robertson 1990). The Elazig–Palu nappe includes Yazgan's (1984) Baskil magmatic rocks that consist of Coniacian-Santonian granodiorites, tonalites, quartz monzonites, monzodiorites, diorites and gabbros of an island-arc. These arc rocks intrude the oceanic rocks and mafic extrusives of the Ispendere–Kömürhan ophiolites of Yazgan (1984) and the Guleman nappe of Michard *et al.* (1984). The Ispendere ophiolite is unconformably overlain by a flysch deposit, which contains fossils of Upper Campanian–Lower Maastrichtian age (Yazgan 1984). The Kömürhan ophiolite structurally beneath the Ispendere ophiolite contains highly deformed, amphibolite-grade mafic, ultramafic and intermediate rocks. The metamorphic rocks are intruded by diorites and granodiorites of the Baskil arc complex (Elazig–Palu nappe). The Guleman ophiolite constitutes the eastern extension of the Ispendere–Kömürhan ophiolite and is in tectonic contact with the Bitlis metamorphic massif. The contact relationships indicate, in general, that the oceanic rocks of the Ispendere–Kömürhan ophiolites and the Guleman nappe form the oceanic basement on which the volcanic arc rocks of the Elazig-Palu nappe (including the Baskil arc) were deposited (Dilek & Moores 1990).

In the eastern part of the East Anatolian High Plateau the Bitlis massif is tectonically overlain to the north and west by the Gevas and Guleman ophiolites, respectively. The Gevas ophiolite, exposed in an east–west trending narrow belt immediately south of Lake Van (Fig. 12), consists of serpentinized ultramafic rocks, cumulate and isotropic gabbros, microgabbros and plagiogranites overlain by extrusive rocks and pelagic sediments (Dilek 1979). These mafic–ultramafic rocks tectonically rest on the Bitlis massif along a south-vergent thrust fault. This thrust fault and the Gevas ophiolite are further deformed and thrust over by the Bitlis massif along north-vergent faults that are depositionally overlain by Palaeocene–Eocene flysch deposits (Dilek 1979).

Mafic–ultramafic rocks and extrusives of similar character crop out farther west, south of the East Anatolian Fault and west of the Bitlis massif, where the Guleman ophiolite overlies tectonically the metamorphosed carbonates of the Bitlis massif (Fig. 11). The Guleman ophiolite includes serpentinized peridotites, banded gabbro, microgabbro, metamorphosed basalt, tuff and agglomerate and radiolarian mudstone (Göncüoglu & Turhan 1984; Aktas & Robertson 1990). The Upper Jurassic–Lower Cretaceous Guleman ophiolite is separated from the underlying Bitlis massif by an intensely mylonitized zone and overlain by an unmetamorphosed Upper Maastrichtian flysch deposit that contains blocks of both the Guleman ophiolite and the Bitlis massif. This depositional relationship constrains the ophiolite emplacement age as pre-late Maastrichtian. The rocks of the Gevas–Guleman ophiolite belt continue farther west and are intruded and overlain by the calc-alkaline intrusives and volcaniclastic rocks of the Elazig–Palu nappe (Ozkaya 1978; Michard *et al.* 1984; Aktas & Robertson 1990).

The Bitlis massif is underlain to the south by a late Cretaceous–early Tertiary tectonic mélange, which directly overlies the foreland deposits of Arabian plate (Fig. 12). The mélange is composed of ophiolitic material tectonically interleaved with hemipelagic and clastic rocks (Aktas & Robertson 1990). In places, however, the Bitlis massif is underlain by thrust sheets of ophiolitic rocks consisting of serpentinized peridotites, gabbro, diabase and basaltic andesites that structurally overlie the tectonic mélange. Both the mélange and the ophiolitic thrust sheets constitute the Killan Imbricate Unit of Aktas and Robertson (1990) that comprises, with the Guleman ophiolite, their Maden complex (Fig. 12). The Maden complex and the overlying Elazig–Palu nappe directly rest on the Arabian platform units along south-vergent thrust faults wherever the Bitlis massif is absent (Dilek & Moores 1990). South of the Bitlis Suture Zone, the lower Palaeozoic to Miocene shelf sequences of the Arabian foreland display a south-vergent fold-and-thrust belt architecture.

East-southeast of the Bitlis massif, south-vergent thrust sheets composed of a complete ophiolite sequence (the Cilo ophiolite) and arc-related calc-alkaline rocks rest tectonically on the Mesozoic Arabian platform (Yilmaz 1985). The Cilo ophiolite contains, from bottom to top, peridotites, cumulate and isotropic gabbros, diorite, quartz diorite, sheeted dykes, pillow and massive lava flows, and ribbon cherts and shales (Yilmaz 1985). The sedimentary rocks associated with the ophiolite give Jurassic to Upper Cretaceous fossil ages; the entire ophiolitic sequence is depositionally overlain by volcanic-pyroclastic rocks and is intruded by granitic–granodioritic intrusions (Fig. 11; Yilmaz 1985). The lower thrust sheet underlying the Cilo ophiolite consists mainly of calc-alkaline lavas, pyroclastics, and blocks of radiolarian chert and recrystallized limestone. These relations suggest that the Cilo ophiolite may constitute the oceanic basement of an ensimatic arc complex represented by the calc-alkaline intrusions and volcanic-pyroclastic rocks.

Deformation and volcanism in the East Anatolian High Plateau

Emplacement of the Tethyan ophiolites in the late Cretaceous and the subsequent continental collisions in the Eocene and mid-Miocene played a major role in the construction of the East Anatolian High Plateau. North–South shortening and crustal imbrication via thrust faulting and folding in the collision zone took up much of the convergence between Arabia and Eurasia. East–West-oriented thrust faults and folds in the Upper Miocene lavas and pyroclastic rocks of the Solhan volcanic rocks in the Mus basin area (Fig. 11; Yilmaz *et al.* 1987) indicate that crustal shortening continued after the Arabia-Eurasia collision and affected the post-collisional volcanic rocks in the plateau. However, progressive thickening of the crust has been accompanied by major strike-slip faulting on the dextral North Anatolian and the sinistral East Anatolian faults that have accommodated the westward escape of the Anatolian plate at a rate of 0.5 cm a^{-1} (Jackson & McKenzie 1984). NE- and NW-striking conjugate strike-slip faults (sinistral and dextral, respectively) with a significant compressional component also occur within the plateau (i.e. Tutak fault; Fig. 11), and some of these faults are seismically active (Tan & Taymaz 2006).

The widespread volcanism in the Turkish–Iranian Plateau started between 8 and 6 Ma, 4–5 Ma years after the initial collision of Arabia with Eurasia in Serravallian-Tortonian times (Innocenti *et al.* 1982; Yilmaz *et al.* 1987; Pearce *et al.* 1990). In general, volcanism in the southern segment of the plateau is characterized by the construction of stratovolcanoes with significant peaks (i.e. Nemrut, Suphan, Tendürek, Ararat; Fig. 11), whereas in the north it forms an extensive (5000 km^2) and relatively flat volcanic field (Erzurum-Kars plateau; Fig. 11) with an average elevation of *c.* 1.5 km above sea level. This volcanic field consists mainly of lava flows intercalated with subordinate ignimbrite units and sedimentary layers giving ages from 6.9 ± 0.9–1.3 ± 0.3 Ma (Innocenti *et al.* 1982; Keskin *et al.* 1998). Pleistocene scoriaceous spatter cones locally overlie this lava-ignimbrite sequence. The initial eruptive phase of post-collisional volcanism in the plateau is characterized by basic and intermediate alkaline rocks and was followed by widespread eruptions of andesitic to dacitic calc-alkaline magma during the Pliocene; the last volcanic phase involved the eruption of alkaline and transitional lavas throughout the Plio-Pleistocene and Quaternary (Yilmaz *et al.* 1987). Most of the major stratovolcanoes in the region were built during this last phase of volcanism, which continued until historical times. Alkaline basaltic lavas of the late volcanic phase appear to predominate mainly in the northern part of the plateau, whereas the calc-alkaline rocks of the second major volcanic phase occur most extensively in the south.

The East Anatolian High Plateau has undergone significant uplift since the Arabian collision in the Mid-Miocene (*c.* 13 Ma). The Lower to Middle Miocene fossiliferous marine marl and reefal carbonates around Lake Van indicate that

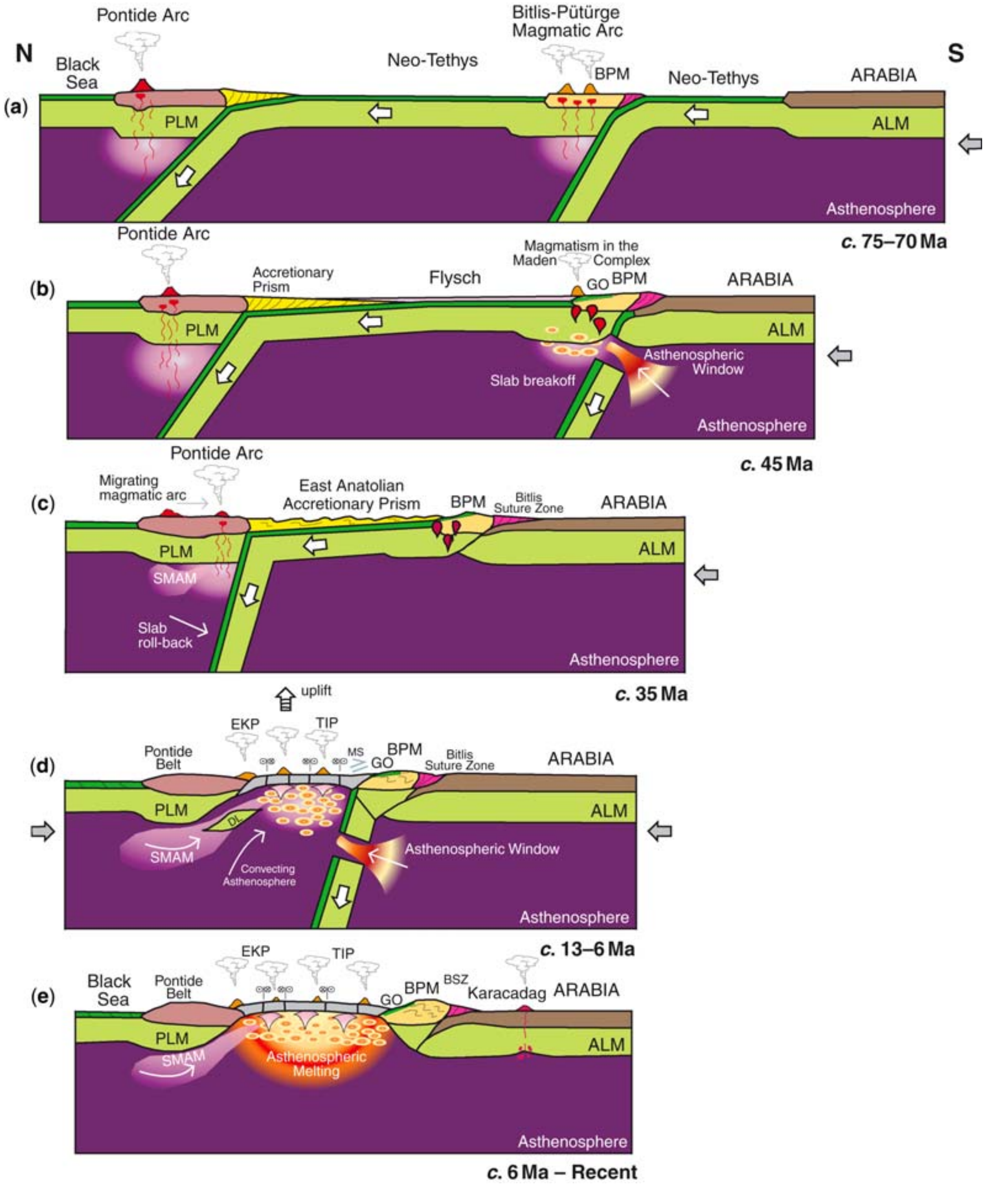

Fig. 13. Maastrichtian–Cenozoic geodynamic evolution of the East Anatolian High Plateau and the subduction-accretion complex through subduction and collisional processes in the upper plate of north-dipping subduction zone(s) within the Tethyan realm (data and interpretations are derived in part from Dilek & Moores 1990; Keskin 2003; Sengör *et al.* 2003; and Dilek *et al.* 2010). Guleman ophiolite (GO) together with the Ispendere–Kömürhan ophiolites and Baskil arc units represent backarc and arc oceanic crust tectonically emplaced onto the northern margin of the Bitlis–Pütürge metamorphic massif by the early Eocene. See text for discussion. Key to lettering: ALM, Arabian lithospheric mantle; BPM, Bitlis–Pütürge massif; BSZ, Bitlis suture zone; EKP, Erzurum–Kars plateau; GO, Guleman ophiolite; MS, Mus suture; PLM, Pontide lithospheric mantle; SMAM, Subduction metasomatized asthenospheric mantle; TIP, Turkish–Iranian high plateau.

the area remained under the sea until the Serravallian (Gelati 1975). Upper Miocene lacustrine and fluvial sedimentary rocks unconformably overlie these marine sedimentary rocks, suggesting the emergence of land and the onset of terrestrial conditions by the late Miocene (Altinli 1966). A late Miocene–early Pliocene erosional surface truncating the fluvial rocks was covered with Pliocene andesitic–dacitic lavas and was subsequently deeply dissected by streams and rivers due to rapid block-uplift of the western and central segments of the plateau (Altinli 1966; Innocenti *et al.* 1976). These stream valleys were then filled with Pleistocene lava flows fed by the alkaline volcanic phase (Erinç 1953).

Tectonic Evolution of the East Anatolian High Plateau

The late Mesozoic geodynamic evolution of eastern Anatolia was controlled by subduction zone tectonics in two separate Tethyan seaways (Fig. 13a). The Northern Tethys seafloor was being consumed at a subduction zone dipping northward beneath the Eastern Pontide arc, and the Black Sea was opening up as a back-arc basin behind this arc around 75–70 Ma (Yilmaz *et al.* 1997). Subduction of the Southern Tethys seafloor beneath the Tauride microcontinent farther south developed a magmatic arc on the Bitlis–Pütürge microcontinent and the arc-backarc oceanic crust presently represented by the Ispendere–Kömürhan and Guleman ophiolites tectonically overlying the Bitlis–Pütürge massifs. A similar tectonic scenario has been suggested for the Cretaceous arc-ophiolite duo in the Malatya–Maras region farther west in the Tauride block (Parlak 2006).

The collision of the Arabian plate with the Bitlis–Pütürge magmatic arc occurred in the early Eocene (Yilmaz 1993) and produced the mélange and flysch deposits along the Bitlis suture zone (Fig. 13b). This continental collision led to slab breakoff and development of an asthenospheric window, which in turn facilitated partial melting of the subduction-metasomatized lithospheric mantle beneath the Bitlis–Pütürge massifs, producing the shoshonitic magmatism in the Maden Complex (Fig. 13b; Elmas & Yilmaz 2003).

Continued subduction of the Northern Tethyan seafloor beneath Eurasia farther north and slab steepening and roll-back produced southward migrating magmatism in the Eastern Pontide arc during the Eocene–Oligocene, while the subduction-accretion complex widened toward the south (Sengör *et al.* 2003). As the Tethyan lithosphere continued its subduction beneath the Pontide arc, the widening East Anatolia accretionary complex was shortened and thickened within the closing basin (Fig. 13c). North–South contraction across the Northern Tethyan realm and vertical thickening of the East Anatolian subduction-accretion complex created a ‘tectonic bumper’ between the converging Eurasia and Bitlis–Pütürge–Arabia plates that had reached the average thickness of continental crust by the late Oligocene–early Miocene (*c.* 24 Ma; Sengör *et al.* 2003). Further steepening and southward retreat of the subducting Tethyan lithosphere might have triggered lithospheric delamination beneath the southern margin of the Eastern Pontide arc and the northern part of the East Anatolian high plateau, resulting in remobilization and partial melting of the subduction-metasomatized asthenospheric mantle (Fig. 13d). This event produced the initial stages of calc-alkaline magmatism in the Erzurum-Kars Plateau by the middle Miocene (Keskin *et al.* 2006).

Arrival of the Bitlis–Pütürge–Arabia composite continental plate at the trench and the continent-trench collision by *c.* 13 Ma slowed down and temporarily arrested the northward subduction beneath the East Anatolian subduction-accretionary complex. However, the continued sinking of the oceanic lithosphere in this subduction zone must have caused the detachment of the subducting slab, leading into slab breakoff and development of an asthenospheric window (Fig. 13d). Rising hot asthenosphere beneath the subduction-accretion complex resulted in widespread partial melting both in the upwelling and convecting asthenosphere and in the overlying crust (Fig. 13d; Sengör *et al.* 2003; Keskin 2003) that produced bimodal volcanism throughout the uplifted plateau. Extensive strike-slip and extensional normal faulting in the Turkish–Iranian high plateau (TIP) facilitated the rise and eruption of asthenosphere-derived alkaline olivine basalts at the surface without much continental contamination in the late Miocene–Pliocene (Fig. 13e).

Widespread volcanism across the entire East Anatolian high plateau (>250 km wide) throughout the late Cenozoic and until historic times indicates a significant heat source beneath it, resulting in extensive melting. The findings of the recent Eastern Turkey Seismic Experiment (ETSE) and tomographic models have shown the lack of mantle lithosphere, an average continental crustal thickness (*c.* 40–45 km), lack of earthquakes deeper than *c.* 30 km, and very low Pn velocity zones indicating the presence of partially molten material beneath the region (Sandvol *et al.* 2003*a*; Al-Lazki *et al.* 2003; Gök *et al.* 2003; Zor *et al.* 2003; Angus *et al.* 2006). These observations collectively suggest that the East Anatolian high plateau is likely supported by hot asthenospheric mantle, not by overthickened crust (Dewey *et al.* 1986) or subducted Arabian continental lithosphere (Rotstein & Kafka 1982) as previously inferred.

Conclusions

The modern Anatolian–African plate boundary is characterized by subduction zone tectonics and is in the initial stages of collision-driven orogenic buildup. The Anatolian microplate itself is made of young orogenic belts (Eocene and younger) that evolved during a series of collisions between Gondwana-derived ribbon continents and trench-roll-back systems within the Tethyan realm. The collision of the Eratosthenes seamount with the Cyprus trench since the late Miocene is a smaller-scale example of this accretionary process and has affected the slab geometry and kinematics of the subducting African lithosphere.

Pn velocity and Sn attenuation tomography results show that the uppermost mantle beneath much of the young orogenic belts in Anatolia is anomalously hot and thin. This is consistent with the surface geology, which is dominantly controlled by strike-slip and extensional tectonics and widespread volcanism in western, central and eastern Turkey. In all these areas, the extension was well under way by the late Oligocene–Miocene, following the main episodes of continental collisions. Pinning of subduction hinge zones by the accreted ribbon continents arrested slab roll-back processes, causing terrane stacking and crustal thickening, and resulted in slab breakoff because of continued convergence of the lithospheric mantle. Slab breakoff-induced asthenospheric upwelling provided the necessary heat and melt to produce the first phases of post-collisional magmatism in these young orogenic belts. Renewed subduction and slab roll-back in the Tethyan realm triggered lithospheric-scale extension in the upper plate, and the thermally weakened orogenic crust started collapsing. These processes resulted in rapid exhumation of recently formed high-pressure metamorphic rocks and in the formation of metamorphic core complexes.

The Cenozoic geodynamic evolution of the western, central and eastern Anatolian orogenic belts indicates that the asthenospheric mantle beneath collision zones responds swiftly to crustal tectonics on time scales of just a few million years. Slab breakoff, lithospheric delamination and slab tearing were common processes that resulted directly from collision-induced events, and caused convective remobilization of the asthenosphere leading to magmatism. Asthenospheric upwelling and partial melting played a major role in a geochemical progression of post-collisional magmatism from initial shoshonitic, calc-alkaline to late-stage alkaline affinities through time.

The collision-driven tectonic evolution of the Anatolian–African plate boundary and the young orogenic belts in the eastern Mediterranean region is typical of the geodynamic development of the Alpine–Himalayan orogenic system. Successive collisions of Gondwana-derived microcontinents with trench-roll-back cycles in the Tethyan realms of the Alpine–Himalayan system caused basin collapse, ophiolite emplacement and continental accretion, producing subparallel mountain belts. Subduction of the Tethyan mantle lithosphere was nearly continuous throughout these accretionary processes, only temporarily punctuated by slab breakoff events.

Part of this study was undertaken during the Eastern Turkey Seismic Experiment (ETSE), which was supported by the NSF under Grant No EAR-9804780; additional support for this experiment was provided by the Bogaziçi University Research Fund under Grant No 99T206. We gratefully acknowledge these grants. The geological fieldwork in Turkey has been funded over the years by the NSF Tectonics Program, Miami University Committee on Faculty Research and Hampton International Initiatives Funds, Scientific & Technical Research Council of Turkey (TUBITAK), and Istanbul Technical University Research Funds. Discussions with S. Altunkaynak, M. Barazangi, E. Bozkurt, C. Genç, R. Gök, C. Helvaci, Y. K. Kadioglu, A. Polat, Y. Savasçin, F. Yagmurlu, Y. Yilmaz, and E. Zor on various aspects of the Mesozoic–Cenozoic geology, geodynamics and seismic structure of Anatolia have been most helpful to us in developing the ideas and interpretations presented in this paper. Thorough and constructive reviews by D. Nance, B. Murphy and P. T. Robinson helped us improve the paper.

References

Agostini, S., Doglioni, C., Innocenti, F., Manetti, P., Tonarini, S. & Savaşçin, M. Y. 2007. The transition from subduction-related to intraplate Neogene magmatism in the Western Anatolia and Aegean area. *In*: Beccaluva, L., Bianchini, G. & Wilson, M. (eds) *Cenozoic Volcanism in the Mediterranean Area*. Geological Society of America Special Paper, **418**, 1–16.

Akay, E. & Erdogan, B. 2004. Evolution of Neogene calc-alkaline to alkaline volcanism in the Aliaga-Foça region (Western Anatolia, Turkey). *Journal of Asian Earth Science*, **24**, 367–387.

Akiman, O., Erler, A., Göncüoğlu, M. C., Guleç, N., Geven, A., Tureli, T. K. & Kadioglu, Y. K. 1993. Geochemical characteristics of granitoids along the western margin of the Central Anatolian Crystalline Complex and their tectonic implications. *Geological Journal*, **28**, 371–382.

Aktas, G. & Robertson, A. H. F. 1990. Tectonic evolution of the Tethys suture zone in SE Turkey: evidence from the petrology and geochemistry of Late Cretaceous and Middle Eocene extrusives. *In*: Malpas, J., Moores, E. M., Panayiotou, A.

& XENOPHONTOS, C. (eds) *Ophiolites, Oceanic Crustal Analogues, Proceedings of the Symposium 'Troodos 1987'*. The Geological Survey Department, Nicosia, Cyprus, 311–328.

ALDANMAZ, E., PEARCE, J. A., THIRWALL, M. F. & MITCHELL, J. 2000. Petrogenetic evolution of late Cenozoic, post-collision volcanism in western Anatolia, Turkey. *Journal of Volcanology & Geothermal Research*, **102**, 67–95.

ALDANMAZ, E., KÖPRÜBASI, N., GÜRER, Ö. F., KAYMAKÇI, N. & GOURGAUD, A. 2006. Geochemical constraints on the Cenozoic, OIB-type alkaline volcanic rocks of NW Turkey: implications for mantle sources and melting processes. *Lithos*, **86**, 50–76.

ALESSANDRINI, B., BERANZOLI, L., DRAKATOS, G., FALCONE, C., KARANTONIS, G., MELE, F. M. & STAVRAKAKIS, G. 1997. Back arc basins and P-wave crustal velocity in the Ionian and Aegean regions. *Geophysical Research Letters*, **24**, 527–530.

ALICI, P., TEMEL, A., GOURGAUD, A., KIEFFER, G. & GÜNDOGDU, M. N. 1998. Petrology and geochemistry of potassic rocks in the Gölcük area (Isparta, SW Turkey): genesis of enriched alkaline magmas. *Journal of Volcanology and Geothermal Research*, **85**, 423–446.

ALICI, P., TEMEL, A. & GOURGAUD, A. 2002. Pb–Nd–Sr isotope and trace element geochemistry of Quaternary extension-related alkaline volcanism: a case study of Kula region (western Anatolia, Turkey). *Journal of Volcanology & Geothermal Research*, **115**, 487–510.

AL-LAZKI, A. I., SEBER, D., SANDVOL, E., TÜRKELLI, N., MOHAMAD, R. & BARAZANGI, M. 2003. Tomographic Pn velocity and anisotropy structure beneath the Anatolian plateau (eastern Turkey) and the surrounding regions. *Geophysical Research Letters*, **30**(24), 8043, doi: 10.1029/2003GL017391.

AL-LAZKI, A. I., SANDVOL, E., SEBER, D., BARAZANGI, M., TÜRKELLI, N. & MOHAMMAD, R. 2004. Pn tomographic imaging of mantle lid velocity and anisotropy at the junction of the Arabian, Eurasian and African plates. *Geophysical Journal International*, **158**, 1024–1040.

ALTINLI, E. 1966. Dogu ve güneydogu Anadolu'nun jeolojisi (in Turkish). *Bulletin of the Mineral Research & Exploration Institute of Turkey*, **66**, 35–74.

ALTUNKAYNAK, Ş. 2004. *Post collisional multistage magmatism in northwest Anatolia (Turkey): Geochemical and isotopic study of Orhaneli magmatic associations*. International Geological Congress, Florence, Italy, August 20–28, 2004. Abstracts 1298.

ALTUNKAYNAK, Ş. 2007. Collision-driven slab breakoff magmatism in northwestern Anatolia, Turkey. *Journal of Geology*, **115**, 63–82.

ALTUNKAYNAK, Ş. & DILEK, Y. 2006. Timing and nature of postcollisional volcanism in western Anatolia and geodynamic implications. *In*: DILEK, Y. & PAVLIDES, S. (eds) *Postcollisional Tectonics and Magmatism in the Mediterranean Region and Asia*. Geological Society of America Special Paper, **409**, 321–351.

ANGUS, D. A., WILSON, D. C., SANDVOL, E. & NI, J. F. 2006. Lithospheric structure of the Arabian and Eurasian collision zone in eastern Turkey from S-wave receiver functions. *Geophysical Journal International*, **166**, 1335–1346.

AYDIN, N. S., GONCUOGLU, M. C. & ERLER, A. 1998. Latest Cretaceous magmatism in the Central Anatolian Crystalline Complex: review of field, petrographic and geochemical features. *Turkish Journal of Earth Sciences*, **7**, 259–268.

BARKA, A. & REILINGER, R. 1997. Active tectonics of the Eastern Mediterranean region: deduced from GPS, neotectonic and seismicity data. *Annali Di Geofisica*, **XL**, 587–610.

BAYHAN, H. 1987. Cefalıkdag ve Baranadag plütonlarının (Kaman) petrografik ve kimyasal-mineralojik özelikleri. *Jeoloji Mühendisligi*, **30–31**, 11–16 (in Turkish).

BIJWAARD, H. & SPAKMAN, W. 2000. Non-linear global P-wave tomography by iterated linearized inversion. *Geophysical Journal International*, **141**, 71–82.

BINGÖL, E., DELALOYE, M. & ATAMAN, G. 1982. Granitic intrusions in Western Anatolia: A contribution of the geodynamic study of this area. *Eclogae Geologica Helvetica*, **75**, 437–446.

BINGÖL, E., DELALOYE, M. & GENÇ, S. 1994. Magmatism of northwestern Anatolia. *International Volcanological Congress, IAVCEI 1994, Excursion Guide (A3)*, 56.

BLUMENTHAL, M. M. 1956. *Yüksek Bolkardaginin kuzey kenar bölgelerinin ve bati uzantilarinin jeolojisi (Güney Anadolu Toroslari)*. Mineral Research and Exploration Institute of Turkey (MTA). Special Publication Series D, **7**, 153.

BOZKURT, E. 2003. Origin of NE-trending basins in western Turkey. *Geodinamica Acta*, **14**, 61–81.

BOZKURT, E. 2004. Granitoid rocks of the southern Menderes Massif (Southwest Turkey): field evidence for Tertiary magmatism in an extensional shear zone. *International Journal of Earth Sciences*, **93**, 52–71.

BOZKURT, E. 2007. Extensional v. contractional origin for the southern Menderes shear zone, SW Turkey: tectonic and metamorphic implications. *Geological Magazine*, **144**, 191–210.

BOZKURT, E. & PARK, R. G. 1994. Southern Menderes Massif: an incipient metamorphic core complex in western Anatolia, Turkey. *Journal of the Geological Society, London*, **151**, 213–216.

BOZKURT, E. & SATIR, M. 2000. The southern Menderes Massif (western Turkey): geochronology and exhumation history. *Geological Journal*, **35**, 285–296.

BOZTUG, D. 2000. S-I-A-type intrusive associations: geodynamic significance of synchronism between metamorphism and magmatism in Central Anatolia, Turkey. *In*: BOZKURT, E., WINCHESTER, J. A. & PIPER, J. D. A. (eds) *Tectonics and Magmatism in Turkey and the Surrounding Area*. Geological Society, London, Special Publications, **173**, 441–458.

BOZTUG, D., DEBON, F., INAN, S., TUTKUN, Z. S., AVCI, N. & KESGIN, Ö. 1997. Comparative geochemistry of four plutons from the Cretaceous–Palaeogene central Anatolian alkaline province (Divrigi region, Sivas, Turkey). *Turkish Journal of Earth Sciences*, **6**, 96–115.

CANDAN, O., ÇETINKAPLAN, M., OBERHÄNSLI, R., RIMMELÉ, G. & AKAL, C. 2005. Alpine high-P/low-T metamorphism of the Afyon Zone and implications for the metamorphic evolution of Western Anatolia, Turkey. *Lithos*, **84**, 102–124.

CATLOS, E. J. & ÇEMEN, I. 2005. Monazite ages and the evolution of the Menderes Massif, western Turkey. *International Journal of Earth Sciences*, **94**, 204–217.

ÇELIK, Ö. F. & CHIARADIA, M. 2008. Geochemical and petrological aspects of dike intrusions in the Lycian ophiolites (SW Turkey): a case study for the dike emplacement along the Tauride Belt Ophiolites. *International Journal of Earth Sciences*, **97**, 1151–1164, doi: 10.1007/s00531-007-0204-0.

ÇELIK, Ö. F., DELALOYE, M. & FERAUD, G. 2006. Precise ^{40}Ar–^{39}Ar ages from the metamorphic sole rocks of the Tauride Belt Ophiolites, southern Turkey: implications for the rapid cooling history. *Geological Magazine*, **143**, 213–227.

ÇEMEN, I., CATLOS, E. J., GÖGÜS, O. & ÖZERDEM, C. 2006. Postcollisional extensional tectonics and exhumation of the Menderes massif in the Western Anatolia extended terrane. *In*: DILEK, Y. & PAVLIDES, S. (eds) *Postcollisional tectonics and magmatism in the Mediterranean region and Asia*. Geological Society of America Special Paper, **409**, 353–379.

ÇOBAN, H. & FLOWER, M. F. J. 2006. Mineral phase compositions in silica-undersaturated 'leucite' lamproites from the Bucak area, Isparta, SW Turkey. *Lithos*, **89**, 275–299.

COLLINS, A. & ROBERTSON, A. H. F. 2003. Kinematic evidence for Late Mesozoic–Miocene emplacement of the Lycian Allochthon over the Western Anatolide Belt, SW Turkey. *Geological Journal*, **38**, 295–310.

CONCEIÇAO, R. V. & GREEN, D. H. 2004. Derivation of potassic (shoshonitic) magmas by decompression melting of phlogopite + pargasite lherzolite. *Lithos*, **72**, 209–229, doi: 10.1016/j.lithos.2003.09.003.

DAVIS, J. H. & VON BLANCKENBURG, F. 1995. Slab breakoff: a model of lithosphere detachment and its test in the magmatism and deformation of collisional orogens. *Earth and Planetary Science Letters*, **129**, 85–102.

DELALOYE, M. & BINGÖL, E. 2000. Granitoids from western and northwestern Anatolia: geochemistry and modeling of geodynamic evolution. *International Geology Review*, **42**, 241–268.

DEMIRTASLI, E., TURHAN, N., BILGIN, A. Z. & SELIM, M. 1984. Geology of the Bolkar Mountains. *In*: TEKELI, O. & GÖNCÜOGLU, M. C. (eds) *Geology of the Taurus Belt, Proceedings of the International Symposium, Geology of the Taurus Belt, 1984*. Ankara, Mineral Research & Exploration Institute of Turkey (MTA), Ankara, 125–141.

DEWEY, J. F., HEMPTON, M. R., KIDD, W. S. F., SAROGLU, F. & SENGÖR, A. M. C. 1986. Shortening of continental lithosphere: the neotectonics of Eastern Anatolia – a young collision zone. *In*: COWARD, M. P. & RIES, A. C. (eds) *Collision Zone Tectonics*. Geological Society, London, Special Publications, **19**, 3–36.

DILEK, Y. 1979. *Geology of Gevas (Van Province, Turkey) and surrounding areas*. Diploma thesis, Institute of Applied Geology, Faculty of Science, Istanbul University, Turkey, 1–63.

DILEK, Y. 2006. Collision tectonics of the Mediterranean region: causes and consequences. *In*: DILEK, Y. & PAVLIDES, S. (eds) *Postcollisional Tectonics and Magmatism in the Mediterranean Region and Asia*. Geological Society of America Special Paper, **409**, 1–13.

DILEK, Y. & ALTUNKAYNAK, S. 2007. Cenozoic crustal evolution and mantle dynamics of post-collisional magmatism in western Anatolia. *International Geology Review*, **49**, 431–453.

DILEK, Y. & ALTUNKAYNAK, S. 2008. Geochemical and temporal evolution of Cenozoic magmatism in western Turkey: mantle response to collision, slab breakoff, and lithospheric tearing in an orogenic belt. *In*: VAN HINSBERGEN, D. J. J., EDWARDS, M. A. & GOVERS, R. (eds) *Collision and Collapse at the Africa-Arabia-Eurasia Subduction Zone*. Geological Society, London, Special Publications, **311**, 213–233, doi: 10.1144/SP311.8.

DILEK, Y. & FLOWER, M. F. J. 2003. Arc-trench roll back and forearc accretion: 2. Model template for Albania, Cyprus, and Oman. *In*: DILEK, Y. & ROBINSON, P. T. (eds) *Ophiolites in Earth History*. Geological Society of London Special Publications, **218**, 43–68.

DILEK, Y. & MOORES, E. M. 1990. Regional Tectonics of the Eastern Mediterranean ophiolites. *In*: MALPAS, J., MOORES, E. M., PANAYIOTOU, A. & XENOPHONTOS, C. (eds) *Ophiolites, Oceanic Crustal Analogues, Proceedings of the Symposium 'Troodos 1987'*. The Geological Survey Department, Nicosia, Cyprus, 295–309.

DILEK, Y. & THY, P. 2006. Age and petrogenesis of plagiogranite intrusions in the Ankara mélange, central Turkey. *Island Arc*, **15**, 44–57.

DILEK, Y. & WHITNEY, D. L. 1997. Counterclockwise *P-T-t* trajectory from the metamorphic sole of a Neo-Tethyan ophiolite (Turkey). *Tectonophysics*, **280**, 295–310.

DILEK, Y. & WHITNEY, D. L. 1998. Syn-metamorphic to neotectonic evolution of the Ecemis strike-slip fault zone (Turkey). *EOS Transactions, American Geophysical Union*, **80**, F915.

DILEK, Y. & WHITNEY, D. L. 2000. Cenozoic crustal evolution in central Anatolia: extension, magmatism and landscape development. *In*: PANAYIDES, I., XENOPHONTOS, C. & MALPAS, J. (eds) *Proceedings of the Third International Conference on the Geology of the Eastern Mediterranean*. Geological Survey Department, September 1998, Nicosia, Cyprus, 183–192.

DILEK, Y., THY, P., HACKER, B. & GRUNDVIG, S. 1999*a*. Structure and petrology of Tauride ophiolites and mafic dike intrusions (Turkey): implications for the Neo-Tethyan ocean. *Bulletin of the Geological Society of America*, **111**, 1192–1216.

DILEK, Y., WHITNEY, D. L. & TEKELI, O. 1999*b*. Links between tectonic processes and landscape morphology in an alpine collision zone, south-central Turkey. *Annals of Geomorphology (Z. Geomorph. N.F.)*, **118**, 147–164.

DILEK, Y., FURNES, H. & SHALLO, M. 2008. Geochemistry of the Jurassic Mirdita ophiolite (Albania) and the MORB to SSZ evolution of a marginal basin oceanic crust. *Lithos*, **100**, 174–209, doi: 10.1016/j.lithos.2007.06.026.

DILEK, Y., IMAMVERDIYEV, N. & ALTUNKAYNAK, S. 2010. Geochemistry and tectonics of Cenozoic volcanism in the Lesser Caucasus (Azerbaijan) and the Peri-Arabian region: Collision-induced mantle dynamics and its magmatic fingerprint. *International Geology Review*, in press.

DOGLIONI, C., AGOSTINI, S., CRESPI, M., INNOCENTI, F., MANETTI, P., RIGUZZI, F. & SAVASÇIN, Y. 2002. On the extension in western Anatolia and the Aegean Sea. *In*: ROSENBAUM, G. & LISTER, G. S. (eds) *Reconstruction of the Evolution of the Alpine-Himalayan Orogen*. Journal of the Virtual Explorer, **8**, 169–183.

DÜZGÖREN-AYDIN, N. S. 2000. Post-collisional granitoid magmatism: case study from the Yozgat Batholith, central Anatolia, Turkey. *Proceedings of the Third International Conference on the Geology of the Eastern Mediterranean*. Geological Survey Department, September 1998, Nicosia, Cyprus, 171–181.

ELITOK, Ö & DRUPPEL, K. 2008. Geochemistry and tectonic significance of metamorphic sole rocks beneath the Beysehir-Hoyran ophiolite (SW Turkey). *Lithos*, **100**, 322–353.

ELMAS, A. & YILMAZ, Y. 2003. Development of an oblique subduction zone-Tectonic evolution of the Tethys suture zone in southeast Turkey. *International Geology Review*, **45**, 827–840. doi: 10.2747/0020-6814.45.9.827.

ERCAN, T., SATIR, M. *ET AL*. 1985. Bati Anadolu Senozoyik volkanitlerine ait yeni kimyasal, izotopik ve radyometrik verilerin yorumu. *Bulletin of the Geological Society of Turkey*, **28**, 121–136 (in Turkish).

ERCAN, T., TURKECAN, A. & KARABIYIKOGLU, M. 1994. *Neogene and Quaternary Volcanics of Cappadocia*. International Volcanological Congress, Ankara, Turkey, 17–22 September 1994, Post Congress Excursion Guidebook, 1–28.

ERDOGAN, B., AKAY, E. & UGUR, M. S. 1996. Geology of the Yozgat region and evolution of the collisional Çankiri basin. *International Geology Review*, **38**, 788–806.

ERINÇ, S. 1953. Dogu Anadolu Cografyasi. *Istanbul Universitesi Yayini*, 572 (in Turkish).

ERLER, A. & BAYHAN, H. 1995. Orta Anadolu granitoidlerinin genel degerlendirilmesi ve sorunları. *Yerbilimleri*, **17**, 49–67 (in Turkish).

FACCENNA, C., JOLIVET, L., PIROMELLI, C. & MORALLO, A. 2003. Subduction and the depth of convection in the Mediterranean mantle. *Journal of Geophysical Research*, **108**, 2099, doi: 1029/2001JB001690.

FAYON, A. K., WHITNEY, D. L., TEYSSIER, C., GARVER, J. I. & DILEK, Y. 2001. Effects of plate convergence obliquity on timing and mechanisms of exhumation of a mid-crustal terrain, the Central Anatolian Crystalline Complex. *Earth and Planetary Science Letters*, **192**, 191–205.

FLOYD, P. A., GÖNCÜOGLU, M. C., WINCHESTER, J. A. & YALINIZ, K. 2000. Geochemical character and tectonic environment of Neotethyan ophiolitic fragments and metabasites in the Central Anatolian Crystalline Complex, Turkey. *In*: BOZKURT, E., WINCHESTER, J. A. & PIPER, J. D. A. (eds) *Tectonics and Magmatism in Turkey and the Surrounding Area*. Geological Society, London, Special Publications, **173**, 183–202.

FRANCALANCI, L., INNOCENTI, F., MANETTI, P. & SAVASÇIN, M. Y. 2000. Neogene alkaline volcanism of the Afyon-Isparta area, Turkey: petrogenesis and geodynamic implications. *Mineralogy & Petrology*, **70**, 285–312.

GARFUNKEL, Z. 1998. Constraints on the origin and history of the Eastern Mediterranean basin. *Tectonophysics*, **298**, 5–35.

GAUTIER, P., BOZKURT, E., HALLOT, E. & DIRIK, K. 2002. Dating the exhumation of a metamorphic dome: geological evidence for pre-Eocene unroofing of the Nigde massif (Central Anatolia, Turkey). *Geological Magazine*, **139**, 559–576.

GELATI, R. 1975. Miocene marine sequence from Lake Van, eastern Turkey. *Rivista italiana di paleontologia e stratigrafia*, **81**, 477–490.

GERYA, T. V., YUEN, D. A. & MARESCH, W. V. 2004. Thermomechanical modeling of slab detachment. *Earth and Planetary Science Letters*, **226**, 101–116.

GESSNER, K., COLLINS, A. S., RING, U. & GÜNGÖR, T. 2004. Structural and thermal history of poly-orogenic basement: U–Pb geochronology of granitoid rocks in the southern Menderes Massif, western Turkey. *Journal of the Geological Society, London*, **161**, 93–101.

GIANELLI, G., PASERINI, P. & SGUAZZONI, G. 1972. Some observations on mafic and ultramafic complexes north of the Bolkardag (Taurus, Turkey). *Bolletino della Societad Geologica Italiana*, **91**, 439–488.

GÖK, R., TÜRKELLI, N., SANDVOL, E., SEBER, D. & BARAZANGI, M. 2000. Regional wave propagation in Turkey and surrounding regions. *Geophysical Research Letters*, **27**(3), 429–432.

GÖK, R., SANDVOL, E., TÜRKELLI, N., SEBER, D. & BARAZANGI, M. 2003. Sn attenuation in the Anatolian and Iranian plateau and surrounding regions. *Geophysical Research Letters*, **30**(24), doi: 10.1029/2003GL018020.

GÖNCÜOGLU, M. C. & TURHAN, N. 1984. Geology of the Bitlis Metamorphic Belt. *In*: TEKELI, O. & GÖNCÜOGLU, M. C. (eds) *Geology of the Taurus Belt*. Proceedings of the International Symposium, Ankara, Turkey, 1983, 237–244.

GÖNCÜOGLU, M. C., TOPRAK, V., KUSCU, I., ERLER, A. & OLGUN, E. 1991. *Orta Anadolu Masifinin batı bölümünün jeolojisi, Bölüm 1: Güney Kesim*. TPAO (Turkish Petroleum Corporation) Report No. 2909, 134.

GÖRÜR, N., OKTAY, F., SEYMEN, I. & SENGÖR, A. M. C. 1984. Palaeotectonic evolution of the Tuzgölü basin complex, central Turkey: sedimentary record of a Neo-Tethyan closure. *In*: DIXON, J. E. & ROBERTSON, A. H. F. (eds) *Geological Evolution of the Eastern Mediterranean*. Geological Society, London, Special Publications, **17**, 467–482.

GOVERS, R. & WORTEL, M. J. R. 2005. Lithosphere tearing at STEP faults: response to edges of subduction zones. *Earth and Planetary Science Letters*, **236**, 505–523.

GÜLEÇ, N. 1994, Rb–Sr isotope data from the Agaçören granitoid (East of Tuz Gölü): geochronological and genetical implications. *Turkish Journal of Earth Sciences*, **3**, 39–43.

GÜLEÇ, N. & KADIOGLU, Y. K. 1998. Relative involvement of mantle and crustal components in the Agaçören granitoid (central Anatolia-Turkey): estimates from trace element and Sr-isotope data. *Chemie der Erde – Geochemistry*, **58**, 23–37.

GÜRSU, S., GÖNCÜOGLU, M. C. & BAYHAN, H. 2004. Geology and geochemistry of the Pre-early Cambrian rocks in the Sandikli area: implications for the Pan-African evolution of NW Gondwanaland. *Gondwana Research*, **7**, 923–935.

HANSMANN, W. & OBERLI, F. 1991. Zircon inheritance in an igneous rock suite from the southern Adamello batholith (Italian Alps). *Contributions to Mineralogy and Petrology*, **107**, 501–518.

HARRIS, N. B. W., KELLEY, S. & OKAY, A. I. 1994. Post-collisional magmatism and tectonics in northwest Anatolia. *Contributions to Mineralogy and Petrology*, **117**, 241–252.

HELVACI, C. & GRIFFIN, W. L. 1984. Rb–Sr geochronology of the Bitlis massif, Avnik (Bingöl) area, SE Turkey. *In*: DIXON, J. E. & ROBERTSON, A. H. F. (eds) *Geological Evolution of the Eastern Mediterranean*. Geological Society, London, Special Publications, **17**, 403–413.

HETZEL, R. & REISCHMANN, T. 1996. Intrusion age of Pan-African augen gneisses in the southern Menderes Massif and the age of cooling after Alpine ductile extensional deformation. *Geological Magazine*, **133**, 565–572.

ILBEYLI, N. 2004. Petrographic and geochemical characteristics of the Hamit Alkaline Intrusion in the Central Anatolian Crystalline Complex, Turkey. *Turkish Journal of Earth Sciences*, **13**, 269–286.

ILBEYLI, N. 2005. Mineralogical-geochemical constraints on intrusives in central Anatolia, Turkey: tectono-magmatic evolution and characteristics of mantle source. *Geological Magazine*, **142**, 187–207.

ILBEYLI, N., PEARCE, J. A., THIRWALL, M. F. & MITCHELL, J. G. 2004. Petrogenesis of collision-related plutonics in Central Anatolia, Turkey. *Lithos*, **72**, 163–182.

INNOCENTI, F., MAZZUOULI, G., PASQUARE, F., RADICATI DI BROZOLA, F. & & VILLARI, L. 1975. The Neogene calcalkaline volcanism of Central Anatolia: geochronological data on Kayseri-Nigde area. *Geological Magazine*, **112**, 349–360.

INNOCENTI, F., MAZZUOULI, G., PASQUARE, F., RADICATI DI BROZOLA, F. & VILLARI, L. 1976. Evolution of volcanism in the area between the Arabian, Anatolian, and Iranian plates (Lake Van, Eastern Turkey). *Journal of Volcanological and Geothermal Research*, **1**, 103–112.

INNOCENTI, F., MAZZUOULI, G., PASQUARE, F., RADICATI DI BROZOLA, F. & VILLARI, L. 1982. Tertiary and Quaternary volcanism of the Erzurum-Kars area (Eastern Turkey): geochronological data and geodynamic evolution. *Journal of Volcanological and Geothermal Research*, **13**, 223–240.

INNOCENTI, F., AGOSTINI, S., DI VINCENZO, G., DOGLIONI, C., MANETTI, P., SAVAŞÇIN, M. Y. & TONARINI, S. 2005. Neogene and Quaternary volcanism in Western Anatolia: magma sources and geodynamic evolution. *Marine Geology*, **221**, 397–421.

ISIK, V., TEKELI, O. & SEYITOGLU, G. 2004. The $^{40}Ar/^{39}Ar$ age of extensional ductile deformation and granitoid intrusion in the northern Menderes core complex: implications for the initiation of extensional tectonics in western Turkey. *Journal of Asian Earth Sciences*, **23**, 555–566.

JACKSON, J. & MCKENZIE, D. 1984. Active tectonics of the Alpine-Himalayan belt between western Turkey and Pakistan. *Geophysical Journal International*, **77**, 185–264.

JOLIVET, L. 2001. A comparison of geodetic and finite strain pattern in the Aegean, geodynamic implications. *Earth and Planetary Science Letters*, **187**, 95–104.

JOLIVET, L. & BRUN, J.-P. 2008. Cenozoic geodynamic evolution of the Aegean. *International Journal of Earth Sciences*, doi: 10.1007/s00531-008-0366-4.

JOLIVET, L. & FACCENNA, C. 2000. Mediterranean extension and the Africa-Eurasia collision. *Tectonics*, **19**, 1095–1106.

JOLIVET, L., BRUN, J. P., GAUTIER, S., LELLEMAND, S. & PATRIAT, M. 1994. 3-D kinematics of extension in the Aegean from the early Miocene to the present: insight from the ductile crust. *Bulletin de la Societe Geologique de France*, **165**, 195–209.

JOLIVET, L., FACCENNA, C., GOFFÉ, B., BUROV, E. & AGARD, P. 2003. Subduction tectonics and exhumation of high-pressure metamorphic rocks in the Mediterranean orogen. *American Journal of Science*, **303**, 353–409.

KADIOGLU, Y. K., DILEK, Y. & FOLAND, K. A. 2006. Slab breakoff and syncollisional origin of the Late Cretaceous magmatism in the Central Anatolian Crystalline Complex, Turkey. *In*: DILEK, Y. & PAVLIDES, S. (eds) *Postcollisional tectonics and magmatism in the Mediterranean region and Asia*. Geological Society of America Special Paper, **409**, 381–415, doi: 10.1130/2006/2409(19).

KADIOGLU, Y. K., DILEK, Y., GULEÇ, N. & FOLAND, K. A. 2003. Tectonomagmatic evolution of bimodal plutons in the Central Anatolian Crystalline Complex, Turkey. *Journal of Geology*, **111**, 671–690.

KÁRASON, H. 2002. *Constraints on mantle convection from seismic tomography and flow modeling*. PhD thesis, Massachusetts Institute of Technology, Cambridge, USA.

KÁRASON, H. & VAN DER HILST, R. D. 2001. Tomographic imaging of the lowermost mantle with differential times of refracted and defracted core phases (PKP, Pdiff). *Journal of Geophysical Research*, **106**, 6569–6587.

KEMPLER, D. & BEN-AVRAHAM, Z. 1987. The tectonic evolution of the Cyprean Arc. *Annales Tectonicae*, **1**, 58–71.

KESKIN, M. 2003. Magma generation by slab steepening and breakoff beneath a subduction-accretion complex: an alternative model for collision-related volcanism in Eastern Anatolia, Turkey. *Geophysical Research Letters*, **30**, 8046, doi: 10.1029/2003GL018019.

KESKIN, M., PEARCE, J. A. & MITCHELL, J. G. 1998. Volcano-stratigraphy and geochemistry of collision-related volcanism on the Erzurum-Kars Plateau, North Eastern Turkey. *Journal of Volcanology and Geothermal Research*, **85**, 355–404.

KESKIN, M., PEARCE, J. A., KEMPTON, P. D. & GREENWOOD, P. 2006. Magma-crust interactions and magma plumbing in a postcollisional setting: geochemical evidence from the Erzurum-Kars volcanic plateau, eastern Turkey. *In*: DILEK, Y. & PAVLIDES, S. (eds) *Postcollisional tectonics and magmatism in the Mediterranean region and Asia*. Geological Society of America Special Paper, **409**, 475–505.

KÖKSAL, S., ROMER, R. L., GÖNCÜOGLU, M. C. & TOKSOY-KÖKSAL, F. 2004. Timing of post-collisional H-type to A-type granitic magmatism: U–Pb titanite ages from the Alpine central Anatolian granitoids (Turkey). *International Journal of Earth Sciences (Geologische Rundschau)*, **93**, 974–989.

KÖPRÜBASI, N. & ALDANMAZ, E. 2004. Geochemical constraints on the petrogenesis of Cenozoic I-type granitoids in Northwest Anatolia, Turkey: evidence for magma generation by lithospheric delamination in a post-collisional setting. *International Geology Review*, **46**, 705–729.

KUMRAL, M., ÇOBAN, H., GEDIKOGLU, A. & KILINÇ, A. 2006. Petrology and geochemistry of augite trachytes and porphyritic trachytes from the Gölcük volcanic region, SW Turkey: a case study. *Journal of Asian Earth Sciences*, **27**, 707–716.

LE PICHON, X. & ANGELIER, J. 1979. The Hellenic arc and trench system: a key to the evolution of the Eastern Mediterranean area. *Tectonophysics*, **60**, 1–42.

LE PICHON, X., LALLEMANT, S. J., CHAMOT-ROOKE, N., LEMEUR, D. & PASCAL, G. 2003. The Mediterranean Ridge backstop and the Hellenic nappes. *Marine Geology*, **186**, 111–125.

LIU, M., CUI, X. & LIU, F. 2004. Cenozoic rifting and volcanism in eastern China: a mantle dynamic link to the Indo-Asian collision? *Tectonophysics*, **393**, 29–42, doi: 10.1016/j.tecto.2004.07.029.

MAURY, R. C., FOURCADE, S. *ET AL*. 2000. Post-collisional Neogene magmatism of the Mediterranean Maghreb margin: a consequence of slab breakoff. *Earth and Planetary Sciences*, **331**, 159–173.

MCCLUSKY, S., BALASSANIAN, S. *ET AL*. 2000. Global Positioning System constraints on plate kinematics and dynamics in the eastern Mediterranean and Caucasus. *Journal of Geophysical Research*, **105**, 5695–5719.

MICHARD, A., WHITECHURCH, H., RICOU, L.-E., MONTIGNY, R. & YAZGAN, E. 1984. Tauric subduction (Malatya-Elazig provinces) and its bearing on tectonics of the Tethyan realm in Turkey. *In*: DIXON, J. E. & ROBERTSON, A. H. F. (eds) *The Geological Evolution of the Eastern Mediterranean Region*. Geological Society, London, Special Publications, **17**, 361–374.

MO, X., ZHAO, Z. *ET AL*. 2006. Petrology and geochemistry of postcollisional volcanic rocks from the Tibetan plateau: implications for lithospheric heterogeneity and collision-induced asthenospheric mantle flow. *In*: DILEK, Y. & PAVLIDES, S. (eds) *Postcollisional tectonics and magmatism in the Mediterranean region and Asia*. Geological Society of America Special Paper, **409**, 507–530.

MOLNAR, P. & OLIVER, J. 1969. Lateral variations of attenuation in the upper mantle and discontinuities in the lithosphere. *Journal of Geophysical Research*, **74**, 2648–2682.

NEMCOK, M., POSPISIL, L., LEXA, J. & DONELICK, R. A. 1998. Tertiary subduction and slab break-off model of the Carpathian-Pannonian region. *Tectonophysics*, **295**, 307–340.

OBERHANSLI, R., BOUSQUET, R. & CANDAN, O. 2008. *Bitlis Massif – East Anatolia Plateau connection?* IGC-33, Session T-18, Oslo-Norway, August 2008.

OKAY, A. I. 1984. Distribution and characteristics of the northwest Turkish blueschists. *In*: DIXON, J. E. & ROBERTSON, A. H. F. (eds) *The Geological Evolution of the Eastern Mediterranean Region*. Geological Society, London, Special Publications, **17**, 455–466.

OKAY, A. I. 2002. Stratigraphic and metamorphic inversions in the central Menderes massif. A new structural model. *International Journal of Earth Sciences*, **91**, 173–178.

OKAY, A. I. & SATIR, M. 2000. Coeval plutonism and metamorphism in a latest Oligocene metamorphic core complex in northwest Turkey. *Geological Magazine*, **137**, 495–516.

OKAY, A. I., SATIR, M., MALUSKI, H., SIYAKO, M., MONIE, P., METZGER, R. & AKYÜZ, S. 1996. Paleo- and Neo-Tethyan events in northwest Turkey: geological and geochronological constraints. *In*: YIN, A. & HARRISON, M. T. (eds) *Tectonics of Asia*. Cambridge University Press, 420–441.

OKAY, A. I., HARRIS, N. B. W. & KELLEY, S. P. 1998. Exhumation of blueschists along a Tethyan suture in northwest Turkey. *Tectonophysics*, **285**, 275–299.

ÖNEN, P. 2003. Neotethyan ophiolitic rocks of the Anatolides of NW Turkey and comparison with Tauride ophiolites. *Journal of the Geological Society, London*, **160**, 947–962.

ONER, Z. & DILEK, Y. 2007. Depositional and tectonic evolution of the Late Cenozoic Alasehir supradetachment basin, western Anatolia (Turkey). *Geological Society of America Abstracts with Programs*, **39**(6), 228.

ÖNEN, A. P. & HALL, R. 1993. Ophiolites and related metamorphic rocks from the Kütahya region, northwest Turkey. *Geological Journal*, **28**, 399–412.

ÖZER, S., SÖZBILIR, H., ÖZKAR, I., TOKER, V. & SARI, B. 2001. Stratigraphy of Upper Cretaceous-Palaeogene sequences in the southern and eastern Menderes Massif (Western Turkey). *International Journal of Earth Sciences*, **89**, 852–866.

ÖZGÜL, N. 1976. Some geological aspects of the Taurus orogenic belt (Turkey). *Bulletin of the Geological Society of Turkey*, **19**, 65–78.

ÖZGÜL, N. 1984. Stratigraphy and tectonic evolution of the Central Taurides. *In*: TEKELI, O. & GÖNCÜOĞLU, M. C. (eds) *Geology of the Taurus Belt, Proceedings of the International Symposium on the Geology of the Taurus Belt, 1983*. Ankara, Turkey, Mineral Research and Exploration Institute of Turkey, Ankara, 77–90.

ÖZGÜL, N. & TURSUCU, A. 1984. Stratigraphy of the Mesozoic carbonate sequence of the Munzur Mountains (Eastern Taurides). *In*: TEKELI, O. & GÖNCÜOĞLU, M. C. (eds) *Geology of the Taurus Belt. Proceedings of the International Symposium, Geology of the Taurus Belt, 1984*. Ankara, Mineral Research & Exploration Institute of Turkey (MTA), Ankara, 173–180.

Özkaya, I. 1978. Stratigraphy of Ergani-Maden area, SE Turkey. *Bulletin of the Geological Society of Turkey*, **21**, 129–139.

Pamic, J., Balen, D. & Herak, M. 2002. Origin and geodynamic evolution of Late Paleogene magmatic associations along the Periadriatic-Sava-Vardar magmatic belt. *Geodinamica Acta*, **15**, 209–231.

Parlak, O. 2006. Geodynamic significance of granitoid magmatism in the southeast Anatolian orogen: geochemical and geochronological evidence from Göksun-Afsin (Kahramanmaras, Turkey) region. *International Journal of Earth Sciences*, **95**, 609–627.

Parlak, O. & Delaloye, M. 1999. Precise ^{40}Ar-^{39}Ar ages from the metamorphic sole of the Mersin ophiolite (Southern Turkey). *Tectonophysics*, **301**, 145–158.

Parlak, O., Delaloye, M. & Bingöl, E. 1996. Mineral chemistry of ultramafic and mafic cumulates as an indicator of the arc-related origin of the Mersin ophiolite (southern Turkey). *Geologische Rundschau*, **85**, 647–661.

Parlak, O., Höck, V. & Delaloye, M. 2002. The supra-subduction zone Pozanti-Karsanti ophiolite, southern Turkey: evidence for high-pressure crystal fractionation of ultramafic cumulates. *Lithos*, **65**, 205–224.

Pasquaré, G., Poli, S., Vezzoli, L. & Zanchi, A. 1988. Continental arc volcanism and tectonic setting in Central Anatolia, Turkey. *Tectonophysics*, **146**, 217–230.

Pearce, J. A. & Bender, J. F. *et al.* 1990. Genesis of collision volcanism in eastern Anatolia, Turkey. *Journal of Volcanology and Geothermal Research*, **44**, 189–229.

Pe-Piper, G. & Piper, D. J. W. 1994. Miocene magnesian andesites and dacites, Evia, Greece: adakites associated with subducted slab detachment and extension. *Lithos*, **31**, 125–140.

Pe-Piper, G. & Piper, D. J. W. 2006. Unique features of the Cenozoic igneous rocks of Greece. *In*: Dilek, Y. & Pavlides, S. (eds) *Postcollisional Tectonics and Magmatism in the Mediterranean Region and Asia*. Geological Society of America Special Paper, **409**, 259–282.

Piromallo, C. & Morelli, A. 2003. P wave tomography of the mantle under the Alpine-Mediterranean area. *Journal of Geophysical Research*, **108**, 2065, doi: 10.1029/2002JB001757.

Purvis, M. & Robertson, A. H. F. 2004. A pulsed extension model for the Neogene-Recent E-W-trending Alasehir Graben and the NE-SW-trending Selendi and Gördes Basins, western Turkey. *Tectonophysics*, **391**, 171–201.

Reilinger, R. E., McClusky, S. C. & Oral, M. B. 1997. Global positioning system measurements of present-day crustal movements in the Arabia-Africa-Eurasia plate collision zone. *Journal of Geophysical Research*, **102**, 9983–9999.

Reilinger, R. E., McClusky, S. C. *et al.* 2006. GPS constraints on continental deformation in the Africa-Arabia-Eurasia continental collision zone and implications for the dynamics of plate interactions. *Journal of Geophysical Research*, **111**, V05411, doi: 10.1029/2005JB004051.

Richardson-Bunbury, J. M. 1996. The Kula volcanic field, western Turkey: the development of a Holocene alkali basalt province and the adjacent normal-faulting graben. *Geological Magazine*, **133**, 275–283.

Ricou, L. E., Argyriadis, I. & Marcoux, J. 1975. L'axe calcaire du Taurus, un alignement de fenetres arabo-africaines sous des nappes radiolaritiques, ophiolitiques et métamorphiques. *Bulletin de la Société de Geologie de France*, **16**, 107–111.

Rimmelé, G., Oberhansli, R., Goffe, B., Jolivet, L., Candan, O. & Çetinkaplan, M. 2003. First evidence of high-pressure metamorphism in the 'Cover Series' of the Southern Menderes Massif. Tectonic and metamorphic implications for the evolution of SW Turkey. *Lithos*, **71**, 19–46.

Ring, U. & Collins, A. S. 2005. U–Pb SIMS dating of synkinematic granites: timing of core-complex formation in the northern Anatolide belt of western Turkey. *Journal of the Geological Society, London*, **162**, 289–298.

Ring, U. & Layer, P. W. 2003. High-pressure metamorphism in the Aegean, eastern Mediterranean: Underplating and exhumation from the Late Cretaceous until the Miocene to Recent above the retreating Hellenic subduction zone. *Tectonics*, **22**(3), 1022, doi: 10.1029/2001TC001350.

Ring, U., Johnson, C., Hetzel, R. & Gessner, K. 2003. Tectonic denudation of a Late Cretaceous-Tertiary collisional belt: regionally symmetric cooling patterns and their relation to extensional faults in the Anatolide belt of western Turkey. *Geological Magazine*, **140**, 421–441.

Robertson, A. H. F. 1998. Tectonic significance of the Eratosthenes Seamount: a continental fragment in the process of collision with a subduction zone in the eastern Mediterranean (Ocean Drilling Program Leg 160). *Tectonophysics*, **298**, 63–82.

Robertson, A. H. F. & Dixon, J. E. 1984. Introduction: aspects of the geological evolution of the eastern Mediterranean: *In*: Dixon, J. E. & Robertson, A. H. F. (eds) *The Geological Evolution of the Eastern Mediterranean*. Geological Society, London, Special Publications, **17**, 1–74.

Rogers, A. J., Ni, J. F. & Hearn, T. M. 1995. Propogation characteristics of short-period Sn And Lg in The Middle East. *Bulletin of The Seismological Society of America*, **87**, 396–413.

Rotstein, Y. & Kafka, A. L. 1982. Seismotectonics of the southern boundary of Anatolia, eastern Mediterranean region; subduction, collision, and arc jumping. *Journal of Geophysical Research*, **87**, 7694–7706.

Russo, R. M., Dilek, Y. & Flower, M. F. J. 2001. Collision-driven mantle flow and crustal response in the eastern Mediterranean region during the late Cenozoic. *4th International Turkish Geology Symposium, Work in Progress on the Geology of Turkey and Its Surroundings*. Adana, Turkey, 24–28 September 2001, 98.

Sandvol, E., Al-Damegh, K. *et al.* 2001. Tomographic imaging of Lg and Sn Propagation in the Middle East. *Pure and Applied Geophysics*, **158**, 1121–1163.

Sandvol, E., Türkelli, N. & Barazangi, M. 2003*a*. The Eastern Turkey Seismic Experiment: the study of a young continent-continent collision. *Geophysical Research Letters*, **30**(24), doi: 10.1029/2003GL018912.

Sandvol, E., Türkelli, N. *et al.* 2003*b*. Shear wave splitting in a young continent-continent collision: an example from eastern Turkey. *Geophysical Research Letters*, **30**(24), doi: 10.1029/2003GL017390.

Saroglu, F., Emre, Ö & Kusçu, I. 1992. *Active fault map of Turkey* (3 sheets, 1:100,000 scale). General Directorate of Mineral Research and Exploration, MTA, Ankara, Turkey.

Savasçin, M. Y. & Oyman, T. 1998. Tectono-magmatic evolution of alkaline volcanics at the Kirka-Afyon-Isparta structural trend, SW Turkey. *Turkish Journal of Earth Sciences*, **7**, 201–214.

Schliestedt, M., Altherr, R. & Matthews, A. 1987. Evolution of the Cycladic Crystalline Complex: petrology, isotope geochemistry and geochronology. *In*: Helgeson, H. C. (ed.) *Chemical Transport in Metasomatic Processes*. Reidel, Dordrecht, 389–428.

Seghedi, I., Downes, H. *et al.* 2004. Neogene-Quaternary magmatism and geodynamics in the Carpathian-Pannonian region: a synthesis. *Lithos*, **72**, 117–146, doi: 10.1016/j.lithos.2003.08.006.

Sengör, A. M. C. & Yilmaz, Y. 1981. Tethyan evolution of Turkey, a plate tectonic approach. *Tectonophysics*, **75**, 181–241.

Sengör, A. M. C., Özeren, S., Genç, T. & Zor, E. 2003. East Anatolian high plateau as a mantle-supported, north-south shortened domal structure. *Geophysical Research Letters*, **30**, 8045, doi: 10.1029/2003GL017858.

Seyitoglu, G., Anderson, D., Nowell, G. & Scott, B. 1997. The evolution from Miocene potassic to Quaternary sodic magmatism in western Turkey: implications for enrichment processes in the lithospheric mantle. *Journal of Volcanology and Geothermal Research*, **76**, 127–147.

Seymen, I. 1984. Kırsehir metamorfitlerinin jeolojik evrimi: Ketin Simpozyumu. *Türkiye Jeoloji Kurumu Yayını*, 133–148 (in Turkish).

Sherlock, S., Kelley, S. P., Inger, S., Harris, N. & Okay, A. I. 1999. ^{40}Ar-^{39}Ar and Rb–Sr geochronology of high-pressure metamorphism and exhumation history of the Tavsanli Zone, NW Turkey. *Contributions to Mineralogy and Petrology*, **137**, 46–58.

Spakman, W., Wortel, M. J. R. & Vlaar, N. J. 1988. The Hellenic subduction zone: a tomographic image and its geodynamic implications. *Geophysical Research Letters*, **15**, 60–63.

Spakman, W., Van Der Lee, S. & Van Der Hilst, R. 1993. Travel-time tomography of the European-Mediterranean mantle down to 1400 km. *Physics of the Earth and Planetary Interiors*, **79**, 3–74.

Tan, O. & Taymaz, T. 2006. Active tectonics of the Caucasus: Earthquake source mechanisms and rupture histories obtained from inversion of teleseismic body waveforms. *In*: Dilek, Y. & Pavlides, S. (eds) *Postcollisional Tectonics and Magmatism in the Mediterranean Region and Asia*. Geological Society of America Special Paper, **409**, 531–578.

Tankut, A., Dilek, Y. & Önen, P. 1998. Petrology and geochemistry of the Neo-Tethyan volcanism as revealed in the Ankara Melange, Turkey. *Journal of Volcanological & Geothermal Research*, **85**, 265–284.

Tatar, M., Hatzfeld, D., Martinod, J., Walpersdorf, A., Ghafori-Ashtiany, M. & Chéry, J. 2002. The present day deformation of the central Zagros from GPS measurements. *Geophysical Research Letters*, **29**, 1927, doi: 10.1029/2002GL015427.

Tekeli, O. 1981. Subduction complex of pre-Jurassic age, northern Anatolia, Turkey. *Geology*, **9**, 68–72.

Thomson, S. N. & Ring, U. 2006. Thermochronologic evaluation of postcollision extension in the Anatolide orogen, western Turkey. *Tectonics*, **25**, TC3005, doi: 10.1029/2005TC001833.

Toprak, V., Keller, J. & Schumacher, R. 1994. *Volcano-tectonic features of the Cappadocian Volcanic Province*. International Volcanological Congress, Ankara, Turkey, 17–22 September 1994, Post Congress Excursion Guidebook, 58.

Van Der Kaaden, G. 1966. The significance and distribution of glaucophane rocks in Turkey. *Bulletin of the Mineral Research and Exploration Institute of Turkey*, **67**, 37–67.

Van Hinsbergen, D. J. J., Hafkenscheid, E., Spakman, W., Meulenkamp, J. E. & Wortel, R. 2005. Nappe stacking resulting from subduction of oceanic and continental lithosphere below Greece. *Geology*, **33**, 325–328.

Von Blanckenburg, F. & Davies, J. H. 1995. Slab breakoff: a model for syncollisional magmatism and tectonics in the Alps. *Tectonics*, **14**, 120–131.

Wdowinski, S., Be-Avraham, Z., Arvidsson, R. & Ekström, G. 2006. Seismotectonics of the Cyprian Arc. *Geophysical Journal International*, **164**, 176–181.

Westaway, B. 1994. Present-day kinematics of the Middle East and eastern Mediterranean. *Journal of Geophysical Research*, **99**, 12071–12090.

Whitney, D. L. & Dilek, Y. 1997. Core complex development in central Anatolia, Turkey. *Geology*, **25**, 1023–1026.

Whitney, D. L. & Dilek, Y. 1998. Metamorphism during crustal thickening and extension in central Anatolia: the Nigde metamorphic core complex. *Journal of Petrology*, **39**, 1385–1403.

Whitney, D. L., Teyssier, C., Dilek, Y. & Fayon, A. K. 2001. Metamorphism of the central Anatolian crystalline complex, Turkey: influence of orogen-normal collision vs. wrench-dominated tectonics on *P-T-t*. paths. *Journal of Metamorphic Geology*, **19**, 411–432.

Widiyantoro, S., Van Der Hilst, R. D. & Wenzel, F. 2004. Deformation of the Aegean slab in the mantle transition zone. *International Journal of Tomography & Statistics*, **D04**, 1–14.

Williams, H. M., Turner, S. P., Pearce, J. A., Kelley, S. P. & Harris, N. B. W. 2004. Nature of the source regions for post-collisional, potassic magmatism in southern and northern Tibet from geochemical variations and inverse trace element modelling. *Journal of Petrology*, **45**, 555–607.

Wortel, M. J. R. & Spakman, W. 1992. Structure and dynamics of subducted lithosphere in the Mediterranean region. *Proceedings of the Koninklijke Nederlandse Akademie van Wetenschappen*, **95**, 325–347.

Wortel, M. J. R. & Spakman, W. 2000. Subduction and slab detachment in the Mediterranean-Carpathian region. *Science*, **290**, 1910–1917.

YAGMURLU, F., SAVASÇIN, M. Y. & ERGUN, M. 1997. Relation of alkaline volcanism and active tectonism within the evolution of Isparta Angle, SW Turkey. *Journal of Geology*, **105**, 717–728.

YAZGAN, E. 1984. Geodynamic evolution of the Eastern Taurus region. *In*: TEKELI, O. & GÖNCÜOĞLU, M. C. (eds) *Geology of the Taurus Belt*. Proceedings of the International Symposium, Geology of the Taurus Belt. 1984, Ankara, Mineral Research & Exploration Institute of Turkey (MTA), Ankara, 199–208.

YILMAZ, Y. 1985. Geology of the Cilo ophiolite: an ancient ensimatic island arc fragment on the Arabian platform, SE Turkey. *Ofioliti*, **10**, 457–484.

YILMAZ, Y. 1990. Comparison of young volcanic associations of western and eastern Anatolia under compressional regime; a review. *Journal of Volcanology and Geothermal Research*, **44**, 69–87.

YILMAZ, Y. 1993. New evidence and model on the evolution of the Southeast Anatolia orogen. *Geological Society of America Bulletin*, **105**, 251–271.

YILMAZ, Y. 2002. Tectonic evolution of western Anatolian extensional province during the Neogene and Quaternary. *Geological Society of America Abstracts with Programs*, **34**(6), 179.

YILMAZ, Y., SAROGLU, F. & GÜNER, Y. 1987. Initiation of the neomagmatism in East Anatolia. *Tectonophysics*, **134**, 177–199.

YILMAZ, Y., TÜYSÜZ, O., YIGITBAS, E., GENÇ, S. C. & SENGÖR, A. M. C. 1997. Geology and tectonic evolution of the Pontides. *In*: ROBINSON, A. G. (ed.) *Regional and Petroleum Geology of the Black Sea and Surrounding Region*. AAPG Memoir, **68**, 183–226.

YILMAZ, Y., GENÇ, S. C., KARACIK, Z. & ALTUNKAYNAK, S. 2001. Two contrasting magmatic associations of NW Anatolia and their tectonic significance. *Journal of Geodynamics*, **31**, 243–271.

ZITTER, T. A. C., WOODSIDE, J. M. & MASCLE, J. 2003. The Anaximander Mountains: a clue to the tectonics of Southwest Anatolia. *Geological Journal*, **38**, 375–394, doi: 10.1002/gj.961.

ZOR, E., SANDVOL, E., GÜRBÜZ, C., TÜRKELLI, N., SEBER, D. & BARAZANGI, M. 2003. The crustal structure of the East Anatolian plateau (Turkey) from receiver functions. *Geophysical Research Letters*, **30**(24), TUR7.1–TUR7.4, doi: 10.1029/2003GL018192.